SEARCH FOR MULTI-PHOTON EVENTS FROM pp INTERACTIONS AT 300 GeV/c

by

Donald Meade Stevens

Dissertation submitted to the Graduate Faculty of the
Virginia Polytechnic Institute and State University
in partial fulfillment of the requirements for the degree of
DOCTOR OF PHILOSOPHY
in
Physics

APPROVED:

G.B. Collins, Chairman

R.L. Bowden

M.C. Li

L.D. Roper

R.F. Tipsword

December, 1974

Blacksburg, Virginia

Acknowledgements

I am grateful to our collaborators at Brookhaven, Dr. J Fischer and Dr. S. Iwata. I would also like to thank

, and the personnel of the machine shop of the Instrumentation Division at BNL.

At FNAL, I would like to thank Dr. P. Koelher and Dr. H. Haggarty, whose exceptional services resulted in the successful completion of this experiment.

At VPI, the machine shop, supervised by , and the electronics shop, supervised by , designed and constructed many of the components of the experiment. I would especially like to thank Dr. P. Trower, who wrote and executed many of the computer programs, and Dr. J. Ficenec, who has devoted much of his time to the execution and analysis of the experiment.

To my thesis advisor, Dr. G.B. Collins, I which to express my thanks for his guidance and for providing me the opportunity to enjoy investigating a part of nature. His enthusiasm for life and his insight to physics made this experiment an enjoyable experience.

My wife, , provided aid and encouragement through the duration of the experiment and data analysis.

TABLE OF CONTENTS

LIST OF FIGURES

LIST OF FIGURES (Cont)

Chapter I

INTRODUCTION

In 1931 Dirac predicted the existance of magnetic monopoles.[1] Many experimental searches for free magnetic monopoles have been conducted to no avail.[2,3]

Ruderman and Zwanziger have explained these negative results without violating the prediction of Dirac.[4] They point out that the ultra-strong, long range forces between monopoles require that they be produced with relativistic velocities in their own center-of-mass system in order to escape their own self-attraction. However, bremstrahlung processes associated with their production greatly exceed the monopole's rest energy. Thus, except for very high energy interactions, created monopole pairs would annihilate producing more radiation. They estimate that at energies of 10^{13} eV, ~ 100 gamma rays, with laboratory energies of a few hundred MeV to a few GeV would result.

To add support to their model, Ruderman and Zwanziger point to the observation of several anomalous energetic narrow pure photon cosmic ray showers first observed by Schien et al.[5] A review of these five events[6] shows that they are remarkably similar; each contained 10-20 photons, all contained within an angle of 10^{-3} - 10^{-4} r, and each event had a total energy of > 10 GeV. Although the monopole origin of these multi-photon events is a most attractive one, other sources have been suggested. In any event the first step would be to rediscover the Schien type events, leaving it to later investigation to determine if they are due to monopole pairs.

We have searched for these multi-photon events produced in proton-nuclei interactions with incident energy of 300 GeV at the Fermi National Accelerator Laboratory. In order to detect these multi-photons, we used a detector designed and built in a VPI-BNL collaboration. The central problem was to distinguish Schien type multi-photon events from those produced by π^0 mesons. Schien type multi-photons should show higher multiplicities, smaller angular spreads and higher total energies. The apparatus was accordingly designed to show these differences and to be insensitive to the numerous neutrons present with the photons. The description of the apparatus, the method of analysis and presentation of data follow.

In Chapter II we describe the detector and in Chapter III we explain the procedures for analyzing the data. In Chapter IV we present the properties of the observed multi-photon events and point out the discrepancies with known photon sources. In the final chapter we summarize the data and present our interpretation.

The result in brief is that neutron interactions have prevented examining of small angular divergences where Schien type events might be expected to exist. At larger angular divergences the multiplicity and angular distributions are consistent with multi-photons from π^0 mesons. At these larger angular divergences, however, the energy dependence of the multi-photon events does not agree with π^0 meson production.

Chapter II

EXPERIMENTAL DEVICE

This experiment was performed in the M-2 beam line of the Meson Detector Building at Fermi National Accelerator Laboratory utilizing a multiphoton detector developed in a VPI-BNL collaboration. By varying trigger conditions we selectively enhanced high photon multiplicity events which deposited a minimum energy in the detector.

A. Beam and Target

The detector was set up in the 300 GeV/c diffracted proton beam at the Meson Detector Building. At the end of each main ring acceleration period a fraction of the circulating protons were extracted and focused on the meson target, .04 x .04 x 8 in^3 Be. The resulting 300 GeV/c diffractively scattered protons then entered the M-2 beam line where they were transported, collimated and focused by a series of quadrupole and dipole magnets. The proton beam was focused on our target some 1200 feet downstream. At our target the beam had a spot size of 0.1 x 0.1 in^2, horizontal and vertical angular divergences of 0.1 mr, and intensity variable from 10^4 to 10^8 protons per acceleration period.

Our target was 1 x 3/4 x 8 in^3 Be which was rotated with respect to the incident beam so that effective target thicknesses from 0.1 to 0.5 interaction lengths could be realized.

Three bending magnets downstream of the target swept the unscattered proton beam and all produced charged particles from the detector.

Between the last bending magnet and the detector, the charged beam was contained in a three inch o.d. pipe located at 17.5 mr with respect to the incident beam direction. The unbent neutral secondaries were contained in a 14 inch o.d. vacuum pipe. A schematic of the diffracted proton beam line is given in Fig. 1.

The intensity of the proton beam was monitored using a 3.5 x 3.5 in^2 scintillation counter placed at the downstream end of the 3 inch vacuum pipe. A small counter telescope consisting of two 2 x 1 x .5 in^3 scintillation counters was also located next to the detector in order to monitor the back-scattered particles from the beam dump. When the beam intensity saturated the single scintillation counter, the telescope was used to monitor the intensity.

The beam location and spot size were monitored using a set of horizontal and vertical Single Wire Ionization Chambers, SWICS, whose readout chambers were read into a CAMAC system and displayed on a television monitor in the experimental trailer. This display, which was renewed after each main ring cycle, also allowed us to monitor the beam position since the SWICS were surveyed onto position on the beam line. A schematic of the experimental set-up downstream of the target is given in Fig. 2.

B. Multi-Photon Detector

The multi-photon detector seen in Fig. 3 converted individual photons into electron pairs, counted the number of such pairs, and measured the total energy of each multi-photon event. The detector consisted of three vertical 248 wire proportional chambers, an air and

lead glass Cherenkov counter, and a trigger and a veto scintillation counter array. A detailed description of the detector construction and operation is given in Appendix A.

The detector, located 127 ft downstream of the Be target, had a horizontal acceptance of ±4 mr and a vertical acceptance of ±1.6 mr defined by a lead-scintillator sandwich in front of the detector. Events with particles, charged or neutral, outside this defined solid angle were vetoed. Events with charged particles in the acceptance region were vetoed by the scintillation counter preceeding the detector.

To convert photons into electron showers sheets of converter material were sandwiched among the three proportional chambers. The proportional chambers detected the electrons produced, thus allowing us to infer the number of incident photons. Proportional chambers were used because they have good multiparticle efficiency, short dead time which allowed for high beam rates, and good time resolution which virtually eliminated the possibility of recording two separate events simultaneously. The chamber had sense wires every 1/16 inch and the detector system was 127 ft downstream, thus the angular resolution was .04 mr.

Downstream of the proportional chambers was an air Cherenkov counter bracketed by scintillation counters which defined those charged particles produced in the converter and passing through the Cherenkov counter. Cherenkov light produced by electrons above the threshold energy, 400 MeV, was monitored by a photomultiplier tube. The pulse height of the tube was roughly proportional to the number of above thres-

hold electrons passing through the detector. The spherical mirror used to collect and focus Cherenkov light onto the phototube caused any particle produced in the converter material at an angle greater than 2^{o} to the beam line to be rejected. Therefore, low energy photons which produce electron pairs with large angles were discriminated against.

The air Cherenkov was followed with a total conversion Cherenkov counter used to determine the total energy of the photons in an event. It consisted of a piece of lead glass, 2 interaction and 12 radiation lengths long. The pulse height of the photo tubes viewing the lead glass was proportional to the total photon energy of the event. The details of the calibration of this detector are given in Appendix A.

C. Event Selection

The fast logic which selected and recorded events with the appropriate number of electrons and minimum total energy is outlined in Fig. 4. A valid trigger resulted when no charged particle traversed the veto counters surrounding the solid angle of the detector and minimum signals were obtained from both air and lead glass Cherenkov counters. The signal from the air Cherenkov counter when in coincidence with the bracketing counters was fanned into five threshold discriminators indicating that a charged particle was produced in the converter and fired the air Cherenkov. The signal from the lead glass counter when in coincidence with the air counter and its bracketing counters was fanned into five threshold discriminators. These outputs allowed us to monitor different thresholds on the two Cherenkov counters

while not changing the minimum trigger requirements.

D. Data Acquisition

Our nominal trigger required that an event produce approximately three electrons in the converter, pass through the air counter, and deposit a minimum of at least 100 GeV in the lead glass counter. If the criteria were satisfied, a gate signal was generated for the proportional chamber interface. If the signals were in the gate and if there was at least one hit on the third chamber, the three chambers were scanned by the interface and the hit wire numbers were read through a data break into a PDP-8 memory buffer. During the scanning, the interface was in the "busy" mode so that no additional gate signals could be generated. The details of the proportional chamber readout and interface scanning are given in Appendix A.

The interface accepted eight additional bits of data from the air and the lead glass counter discriminators. A high discriminator level indicated a large number of electrons and high total photon energy respectively. Thus, we could trigger on a low air and glass level which optimized the data acquisition rate, but at the same time tag those events which had a high multiplicity or high energy.

The wire identification codes for hits on proportional chamber wires were read serially into separate 12-bit words of the memory buffer, as were the Cherenkov level codes. A typical event would have codes which corresponded to hits on the first, second, and third proportional chambers plus an air Cherenkov level and a lead glass Cherenkov level. Individual events in the buffer were separated by a word of zeroes.

When the 1024 word data buffer was filled, an interrupt signal was generated by the proportional chamber interface which placed it in the busy mode and signaled the computer to service the buffer. The computer then copied the data buffer onto 7-track 556 BPI magnetic tape and incremented the on-line analysis arrays. This action completed, the data were cleared, the interface placed in data acquisition mode, and more data were accepted.

E. On-Line Monitoring

Data were logged through the computer's data break. Thus while data were taken diagnostic displays could be viewed on a storage scope; wire maps (frequency of hits on chamber wires), chamber multiplicity distributions (frequency of single, double, triple, etc., hits), and individual events. Wire maps and multiplicity distributions were updated after every full data buffer. A teletype provided a hard copy of the distributions for future reference. These displays allowed a check on the detector performance and an overview of the data being acquired. Problems with the proportional chambers or the readout system, such as a dead amplifier or a latch which would not reset, were detected quickly. Fig. 5 shows a typical wire map distribution while Fig. 6 shows a typical multiplicity distribution for the three proportional chambers.

F. Off-Line Monitoring

After each data tape had been filled (about every 12 hrs.), it was analysed on the CDC-6600 available at FNAL. Using the large sample of

data, wire maps and multiplicity distributions could be obtained with good statistics. One hundred events were printed on single event wire maps, providing a highly visible sample of data, and allowing us to examine in detail typical high multiplicity events.

Chapter III

DATA ANALYSIS

Approximately 340,000 events were recorded by the multi-photon detector system. The merged data tapes, four in number, contained the event information; hits on each chamber, air Cherenkov levels, and lead glass Cherenkov levels. Data analysis was performed on the VPI IBM 370/165 computer.

The hits on the chambers were caused by charged particles produced in the converter. From these data we had to extract the number and location of the incident neutral particles. When neutrons interacted in the converter, they produced a spray of charged particles with a typical projected opening angle of 60 mr. The spray resulted in the hits on the third chamber being more numerous than those on the second, which in turn was greater than the number on the first chamber. The vertex of the cone represented the point of interaction of the single neutron in the converter.

If high energy photons were converted, they would also produce a spray, but the number of resulting charged particles from each photon would be small and the cone of the shower would be very narrow. Again, the vertex of the cone would represent the point of conversion of the individual photon. If several incident photons converted, several separate narrow cones would be produced.

For events involving the conversion of several photons or neutrons, the charged particle cones frequently overlapped. There would then be an uncertainty in interpreting the number of neutral incident particles.

The procedure adapted was to identify shower cones with charged particles produced parallel to the incident beam. If these parallel charged particles were displaced sideways from one another, their origins in the converter must have been separate and thus separate incident particles. The specific criteria for separate interactions were:

1. The production angle of the charged particle had to be small, less than 10 mr, as indicated by an angular divergence in the chambers of 2 wires or less between the hit on chamber 1 and the hit on chamber 3.

2. Chamber 1 should show a break in the recorded hits of at least 2 wires. This prevented confusion caused by particles produced at large angles, traveling almost parallel to the chambers, and producing a large number of continuous hits on the chamber.

These criteria were conservative and underestimated the number of incident particles. If the incident particles were separated by less than two wires, two or more particles would be recorded as one. If the neutral particle energy was low and produced only wide angle (> 10 mr) charged particles, the interaction would not be counted. If the number of interacting photons exceeded 5 or 6 the multiplicity would probably be underestimated. If these photons were contained within a cone angle less than .6 mr, they would not be resolved and their multiplicity would be counted as 1 or 2. They could be distinguished from low multiplicity events by noting the air Cherenkov level. One or two particles would produce a minimum Cherenkov level while 5 or 6 particles would produce a higher level.

The insensitivity of the criteria to low energy photons was advantagous since we were concerned with events with energies greater than 100 GeV. In part this insensitivity was augmented by the air Cherenkov which would not respond to electron pairs produced at an angle greater than 2^{o}.

Fig. 7 shows typical events with one or two interacting neutral particles. Fig. 8 shows multiplicity of 3 or 4 while Fig. 9 shows those events where the scheme detected 5 or more interacting particles. Lines are drawn to aid the eye and illustrate the application of the criteria for determining the number of incident particles. In order to eliminate the impression that all events were this clean, Fig. 10 shows some events in which the number of interacting particles is questionable. A large number of these confusing events can be eliminated by noting that they are characterized by minimum gas Cherenkov levels, thus there were few forward going high energy charged particles.

The data analysis resulted in reducing each event to the number of interacting neutral particles, their location, and the associated lead glass and air Cherenkov levels.

Chapter IV

PRESENTATION OF THE DATA

We have analysed 80,000 events with neutral particles produced by 300 GeV protons incident on a .15 interaction length Be target. These neutral particles, neutrons and photons, were detected by their interaction in a .125 inch (.56 radiation lengths and .06 collision length) lead sheet used as a converter in the detector.

A known source of the observed photons are neutral mesons. The multiplicity and angular distribution of these photons are discussed in detail in Appendix B. Neutrons may also interact in the detector system and cause hadronic showers which can be mistaken for photon induced showers. The measurement of this neutron induced background and its elimination from the data is discussed in Appendix B.

The multiplicity distribution, as determined by the scheme described in the preceeding chapter, is shown in Fig. 11 in which the neutron background has been eliminated. Since the probability of one photon converting in the detector is 36%, the most probable number of incident photons is much larger than the observed number. Fig. 11 also shows the expected distribution if all of the photons were from neutral meson sources. It is clear that we observe far more high multiplicity events than would be expected from mesons. The inefficiency of the detector in providing a trigger for 1 and 2 photon events has been included in the predicted distribution, giving agreement at low multiplicities.

Since we measure the location of the incident particles in only one direction, we can calculate the projected opening angle of the cone that

contains the incident photons. As seen in Appendix B, photons from mesons should have a broad cone angle. Fig. 12 shows the projected cone angle for different multiplicities. There is a peak for opening angle less than 1 mr and an enchancement at 2.1 mr. The distribution about 2.1 mr is wide and can be explained by photons from mesons. The events with opening angle less than 1 mr will be discussed later.

The angular resolution of the detector system depends on the number of interacting photons. The criteria for identifying photons require there be two wires between showers, thus the angular resolution decreases with increasing multiplicity. Although the chambers may underestimate the number of photons contained in a small cone angle, the air Cherenkov counter would give a truer indication of the number of photons. Fig. 13 shows the cone angle for different multiplicities for those events having an air Cherenkov level indicating 3 or more charged particles triggering the counter. There is still a peak for a cone angle less than 1 mr, indicating large multiplicity photons contained within a very small cone.

Using the center of the cone describing the incident photons, we also calculate the projected production angle of these photon bunches. Fig. 14 shows the production angle for all events as a function of multiplicity. The distribution narrows for higher multiplicity as expected since the defined solid angle required the events to be centered in the detector in order to be detected. The asymmetry for single multiplicity events is probably due to background processes. The higher multiplicities are gaussian about 0^{o}. If we again look at those

events with an air Cherenkov level greater than minimum, we obtain the distributions shown in Fig. 15. The distributions are as expected for photons from pions. For single events we see few effects from background processes.

Since we had five different levels on the lead glass counter, we can measure the multiplicity as a function of energy deposited in the lead glass. The five different levels represent energy deposits of at least 100, 150, 200, 250, and 285 GeV. Fig. 16 shows the frequency of events verses energy for different multiplicities. For multiplicities of 1 and 2, the distributions decrease for high energies as expected. For higher multiplicities, there is a peak at 150 GeV. Fig. 17 shows the distributions for all events with air Cherenkov levels greater than the minimum. There is a peak for all multiplicities at 150 GeV.

The interpretation of these events will be discussed in the following chapter.

Chapter V

CONCLUSIONS

We have observed multi-photon events whose properties are consistent with photons from decaying neutral mesons. We also have a statistically significant sample of events whose multiplicity, energy and angular distributions are not compatable with photons from directly produced mesons.

These unexplained events have a cone angle much smaller than expected (< 1 mr). A plausable explanation for these anomalous events is as follows: Neutrons, produced by protons in the Be target, interact in the veto counter (.5 inch scintillator) producing neutrons and π^{o}'s diffractively. The pions each decay into two photons which we detect. Because the photons are produced only 22 inches from the detector, their cone angle is small. These events are not eliminated by the subtraction of the neutron background data since the photons convert much more efficiently in the lead converter than in the plexiglass converter. We did not anticipate a significant contribution from these processes, consequently, our detector system was not able to discriminate against them.

The energy distributions for different multiplicities peaks at 150 GeV. We have no explanation for this discrepency and we also are not able to explain the difference in expected and observed photon multiplicities at high multiplicity. These facts indicate that further searches for multi-photon events are necessary and the findings of this

experiment should serve as a guide in investigating this largely unexplored area of high energy physics.

Appendix A

MULTI-PHOTON DETECTOR

To detect multi-photon events we used multi-wire proportional chambers, MWPC, with excellent multiparticle efficiency and good time resolution. We combined these MWPC's with an air Cherenkov counter which was sensitive only to high energy particles produced at small angles and a lead glass Cherenkov counter which discriminated against high energy hadronic events.

A. Proportional Chamber Construction

A MWPC, shown schematically in Fig. 18, consisted of a vertical plane of readout wires sandwiched between two horizontal high voltage planes. The active chamber area was 15" x 15".

The chamber was constructed from four fiberglass G-10[7] frames which allowed for ease of repair when wires broke or gas leaks occurred. The frames were bolted together and then bolted to a 42" x 48" x 1/2" aluminum backing plate. The window edges next to the high voltage plane were concave in shape to inhibit breakdown. The backing plate, which had a window 16.5" x 16.5" gave rigidity to the chamber and facilitated mounting of the chamber.

In a chamber the first frame of G-10, 24" x 24" x 1/4", was covered by a 5 mil clear mylar window and had two input gas ports at the bottom of the active area, and 2 output gas ports at the top of the active area. Next was a high voltage plane, 24" x 24" x 3/8" with 20 per inch, 4 mil stainless steel wires[8] which were contact cemented[9] and 2 component

epoxyed.[10] At one end the wires were also soldered to a printed circuit board which fanned the wires into three groups.

High voltage from a regulated power supply[11] in the experimental trailer 120 ft. away was fed through coaxial cable to a high voltage connector mounted on the Al plane. The voltage was then fanned through 120 M Ω resistance to each wire group. A 1/8 inch O-ring groove was cut into the face of the second frame in order to provide a gas-tight fit.

The third frame, 24" x 24" x 3/8", held the vertical sense wires[8], 1 mil stainless steel placed 16 to the inch. Of a total of 248 wires, 4 wires on each side were outside the active area. The wires were secured with contact cement and epoxy, with one end being soldered to a printed circuit board which fanned the wires into 31 - 8 wire groups ending in a multipin connector. Printed circuit cards which amplified the eight individual wires were plugged into the connectors while their amplified outputs were fed through 200' coaxial cables to the experimental trailer. These cables, grouped by 16 wires, were lashed together and covered with a shield to reduce electrical noise and provide ease of handling. The sense wire plane was sealed to the second plane by using an O-ring as described previously.

The fourth frame, 26" x 26" x 1/4", was another high voltage plane. To the back of this plane a 5 mil mylar sheet was glued to provide a back window. This frame also had an O-ring to provide an air tight seal with the third frame.

Wires were soldered using stainless steel solder flux, washed with a neutralizing agent, rinsed with water, then dried using forced air.

Wires were scanned using a high intensity light to remove any dust or dirt adhesion. With the three O-rings in place, the faces of the planes were coated with RTV[12] and the four frames were bolted together before the RTV sealer had cured. The chamber was then bolted to the backing plate, the high voltage cables were connected, and the chamber was ready for testing.

B. Chamber Readout

To reduce noise, the sense wires of the MWPC were operated at a -1.2 V dc bias. The passage of a charged particle close to a sense wire gave rise to a 2-5 mV pulse with a rise time of ~ 100 ns. These signals were amplified and shaped in the transmitter card electronics illustrated in Fig. 19. The transmitter card output, a 1 V signal, 100 ns wide with a d.c. offset of -1.75 V, was carried through 200' shielded coaxial cable to the interface in the experimental trailer. The cable delay was sufficient to allow the fast logic to decide to scan the data.

The signal cables were grouped into 16 wire units each of which fed into a single receiver card whose logic is indicated in Fig. 19. This printed circuit card mounted in the interface took the MWPC signal and determined if it was within a 70 ns gate generated by the fast logic. If the event was accepted a latch was set which could be scanned later.

The interface, which was designed and built by the Instrumentation Division of BNL, scanned all of the MWPC latches and if a latch had been set it stored in a memory buffer of a PDP-8/I the corresponding

wire number. The interface had scalers which provided visual readouts of logic triggers, the number of times at least one latch was set, and the total number of latches set. The details of the construction and operation of the interface will be given elsewhere.[13]

C. Chamber Testing and Performance

After the chamber was mounted on the backing plate, it was flushed for 48 hours with ultra-pure Ar.[14] Positive voltage was applied to the chamber with random breakdowns occurring at ~ 1800 V indicating no edge breakdown or "hot spots" caused by dirt or dust on the wires.

After the breakdown tests, the chamber was flushed with ultra-pure Ar circulated through dimethoxymethane[15] maintained at 0°C. Negative high voltage was applied to the chamber and a β-ray source provided signals on the anode wires of $\geq$ 2 mV with a rise time of ~ 100 ns for a voltage $\leq$ 5100 V. Above this voltage the chamber had random breakdowns.

When the chamber stabilized with respect to breakdown, the transmitter cards were inserted, and cables connected. A 3 1/4" x 3 1/4" x 3/8" scintillation counter was mounted directly behing the chamber and a β-ray source in front. The counter which detected the traversing β-rays provided the fast logic trigger which started the interface gate. The gate was set at 70-80 ns to measure the efficiency and time response of the chamber with high voltage.

The chamber efficiency was high, 99.9%, but only in a very narrow operating range. When the leading edge of the gate signal was delayed with respect to the chamber signal, a large number of coincidences were observed at large time delays. These signals were caused by ions pro-

duced at large distances from the sense wires.

To reduce the out-of time coincidence events to an acceptable 5% level, we added an electro-negative gas, Freon 13B1[14], to capture a portion of the ions produced. Because the gas also eliminated many of the ions needed to produce the needed 1-2 mV signal, the high voltage had to be raised. Fig. 20 shows the chamber efficiency as a function of delay for various amounts of Freon. Fig. 21 shows the high voltage plateau for the chamber with the gas mixture used during the data runs. The Freon caused the efficiency of the chamber to be reduced to 97% which was tolerated as time resolution was ~ 65 ns.

During data runs the chambers were scanned every 48 hours using a motor-driven and remotely controlled source and scintillation counter. We observed wire maps of the chamber as we moved the scanner across the active area of the chambers. The efficiency of the chambers remained unchanged over the period of the experiment, 8 months elapsed time and 800 hours of operation.

Since the source scanner was highly collimated, we measured the spark size for single particles; 97% 1 wire events, 2% events on 2 adjacent wires, and ~ 1% events on 3 or more adjacent wires.

D. Air Cherenkov Counter

The air Cherenkov counter was designed to detect only those electrons produced by high energy photons.

The counter consisted of a 36" x 36" x 36" box with sides, top and bottom of 1/4" Al sheets and front and back of 1/16" Al sheets.

A spherical mirror with a 6' radius collected Cherenkov light and focused it onto a 5" photo tube.[16] The mirror was made from a 24" x 24" x 6" piece of spherically milled styrofoam coated with two-component epoxy.[10] A second layer of epoxy held a 5 mil sheet of aluminized mylar to the styrofoam.

The focusing efficiency of the mirror was checked using a laser aimed parallel to the main axis of the mirror. Over the entire active area of the mirror, the ~ 1/8" diameter laser beam focused on the photo tube with a maximum spot size diameter of 2 inches.

The counter contained air at atmospheric pressure so only electrons with energy greater than 400 MeV produced Cherenkov light. Also electrons produced with an angle greater than 2^{o} from the symmetry axis of the mirror would not be detected because their Cherenkov light was not focused on the tube. Thus, further discrimination against low energy photons was achieved since their resulting electron pairs were typically produced at large angles.

The counter was positioned with the axis of the mirror located on the neutral beam line. It was supported by aluminum legs and 8.5' horizontal rails mounted on the top and bottom of the counter. The MWPC's and converters were mounted on these rails in front of the counter along with various scintillator counters.

The detection efficiency of the counter for single particles was measured by turning off the sweeping magnets in the M-2 diffracted proton beam which allowed the beam to pass directly through the detector. The counter detected only 40% of the single protons seen by the

scintillation counters. The output pulse height of the photo tube was noted. The magnets were turned on and the proton beam was swept clear of the detector. Scintillation counters were then arranged to guarantee that at least two charged particles passed through the counter and the average pulse height was noted. This process was then repeated for higher multiplicity events. The photo tube output was fanned into five threshold discriminators, the lowest level of which was set at the 1 or 2 particle level, which was used in the fast trigger logic for the data acquisition system. The other four discriminators were set to indicate higher multiplicity events, and their outputs were used by the data handler to tag these events.

E. Lead Glass Cherenkov Counter

This Cherenkov counter, a piece of lead glass[17] 18" x 18" x 12", viewed by 2-5" photo tubes[16] was downstream of the air Cherenkov counter. A light tight wooden box containing the counter was placed in the beam line so the beam traversed 12" while the vertical counter acceptance was 8" and the horizontal 18". The photo tubes were mounted side by side along the 12" dimension so they viewed the shower development through the 18" of material.

To calibrate the lead glass counter, the sweeping magnets were turned off, the target removed, and the M-2 beam line tuned for 40 GeV/c particles, mostly electrons and pions. Since there were 12 radiation and 2 collision lengths of lead glass, the electromagnetic showers developed completely while the hadronic shower only started to develop before

exiting. Fig. 22 shows the pulse height spectrum from the sum of the outputs of the photo tubes. The exponential fall off at low energy was produced by hadronic particles. The gaussian distribution at higher energy resulted from the totally absorbed electromagnetic shower. Fig. 23 shows the results of tuning the M-2 beam line for 65, 100 and 200 GeV/c momentum negative particles. Fig. 24 illustrates the linear response of the photo tubes as a function of the energy of the incident electron.

During the data runs the summed output of the two photo tubes were fanned into five threshold discriminators. The lowest discriminator level was set to 100 GeV total shower energy deposit and was used in the fast trigger logic to select events. The other four discriminators were set to progressively higher energies. Events with high shower energy were tagged by the interface, enabling us to select events according to energy.

Appendix B

BACKGROUND PROCESSES

We consider here processes which contribute to the multiplicity distribution of photons from pp interactions. These contributions, which must necessarily be due to neutral particles because of the veto system, arise from the decay of the π^o's and K^o's and their subsequent photon decay and conversion and from neutron interactions in the converter.

A. Pi-Mesons

Neutral pions, which decay into 2 photons, contribute to the photons seen by our multi-photon detector. Fortunately, experiments have been performed with bubble chambers at FNAL which measured the number, energy, and angular distributions of charged pions produced by 300 GeV/c protons.[18] The distributions of neutral pions can be found assuming symmetry of charged and neutral pions.

The minimum opening angle of 2 photons from π^o decay is

$$\theta_{min} = \frac{2m_{\pi o}}{E_{\pi o}} .$$

Thus, under the most favorable conditions, we will see both photons only when $E_{\pi o} \geq 35$ GeV. Fig. 25 shows the multiplicity distribution of photons expected from hadronically produced π^o's. The angular distribution of photons from π^o's should differ from the distribution of the Schien type events. As noted earlier, the Schien events had photons

contained in 1-2 mr, while the photons from π^0's should be distributed more evenly over our solid angle.

B. K-Mesons

Another source of photons are K-mesons which have decay modes

$$K^0_S \rightarrow 2\pi^0 \rightarrow 4\gamma$$

$$K^0_L \rightarrow 3\pi^0 \rightarrow 6\gamma.$$

The neutral decay occurs 32% of the time for the K^0_S, and 22% of the time for the K^0_L. Because the average number of K^0's produced per interacting proton is .66,

$$< n(K^0_S) > = .33 = < n(K^0_L) >$$

$$< n(K^0_S \rightarrow 2\pi^0) > = .11$$

$$< n(K^0_L \rightarrow 3\pi^0) > = .08$$

These numbers should be compared to the average number of pions produced directly in proton interactions[18],

$$< n(\pi^0) > = 3.9.$$

The contribution of the K^0's to the photon spectrum has been included in the multiplicity and angular distributions of photons from directly produced pions.

C. Neutrons

The multiplicity distribution seen by the multi-photon detector could be biased by neutrons which produce hadronic showers in the converter material.

To study the problem of neutrons, we discriminated against photon

interactions by using a converter with small radiation length. A piece of plexiglass, .052 interaction and .06 radiation lengths, was placed in front of the first wire chamber. The multiplicity distribution obtained is shown in Fig. 27. This distribution is due to interacting neutrons as well as converting photons. It should be noted that 91% of these events had a minimum gas Cherenkov level. The neutron events should have mimimum levels since the showers are produced with large angles compared to photons and thus would not be detected by the Cherenkov counter.

During our data runs, we used a sheet of lead, .56 radiation lengths and .062 interaction lengths. The resulting multiplicity distribution is also shown in Fig. 27. To determine the photon multiplicity, we subtracted the plexiglass distribution from the lead converter distribution. This procedure overestimated the hadronic background since the plexiglass distribution contained some photon events.

REFERENCES

1. P.A.M. Dirac, Proc. Roy. Soc. (London) Ser. A 133, 60(1931).
2. D.M. Stevens, Technical Report, VPI-EPP-70-6.
3. D.M. Stevens, Technical Report, VPI-EPP-73-5.
4. M. Ruderman and D. Zwanziger, Phys. Rev. Letters 22, 146(1969).
5. M. Schien, et al, Phys. Rev. 95, 855(1954) and 99, 643(1955).
6. G.B. Collins, et al, Phys. Rev. D 8, 982(1973).
7. Du Pont, 1007 Market St., Wilmington, Deleware.
8. Consolidated Reactive Metals, 115 Hoyt Ave., Mamaroneck, N.Y.
9. Permabond International Corp., 45 West 45th St. New York, N.Y.
10. Epon Epoxy, Miller-Stephenson Chemicals, Route 7, Danbury, Conn.
11. Power Designs Inc., 1700 Shames Drive, Westbury, L.I., N.Y.
12. General Electric Co., Silicon Products Dept., Waterford, N.Y.
13. J. Fischer, et al, Technical Report, Inst. Div., B.N.L. (to be published).
14. Matheson Gas Products, Box 85, E. Rutherford, N.J.
15. Eastman Kodak Co., State St., Rochester, N.Y.
16. Amperex Elec. Corp., Hicksville, N.Y.
17. We would like to thank Dr. DeWire of Cornell University for the loan of the lead glass.
18. F.T. Dao, et al, Phys. Rev. Letters 33, 389(1974).

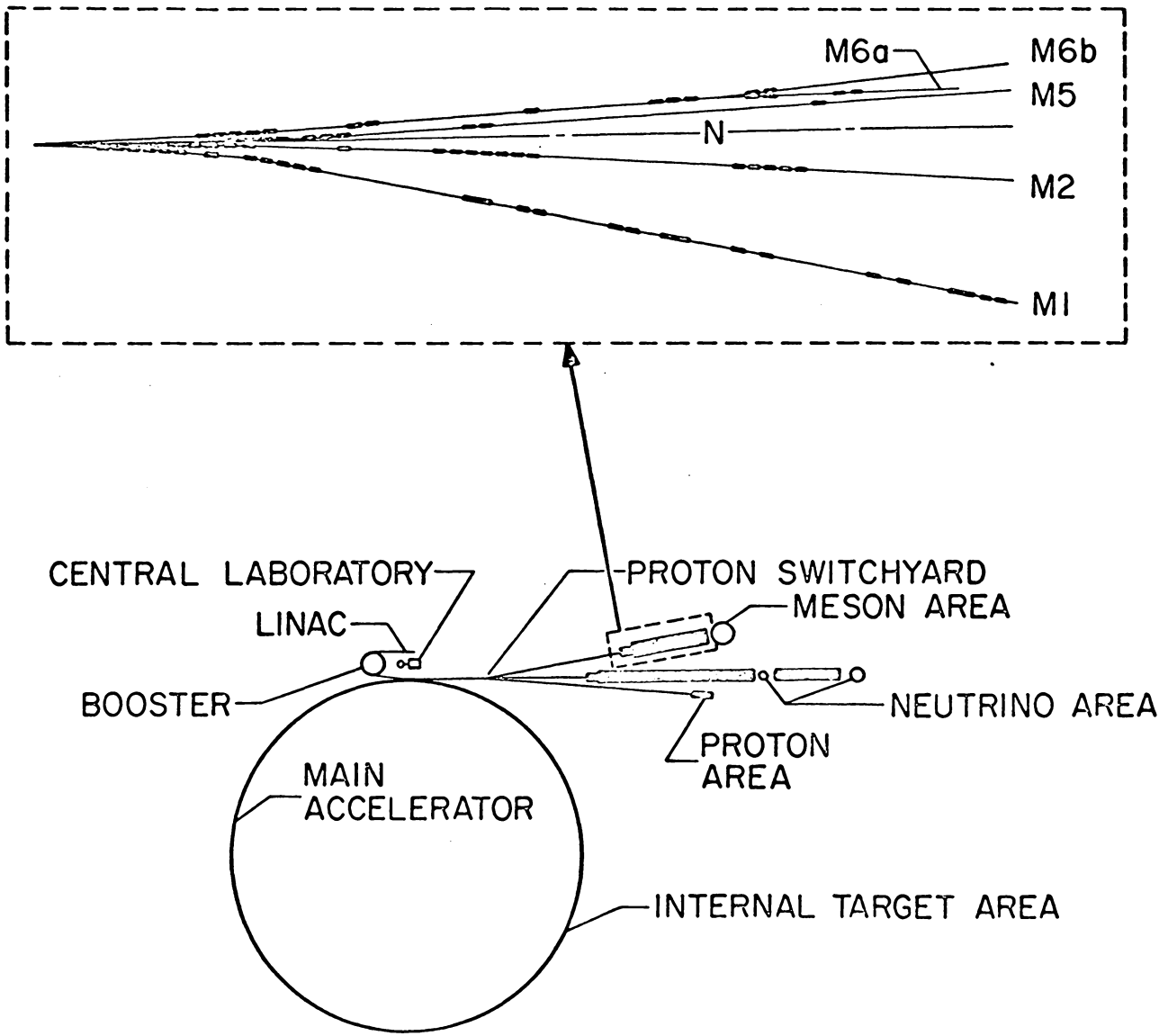

Figure 1. Schematic of Proton Beam Line.

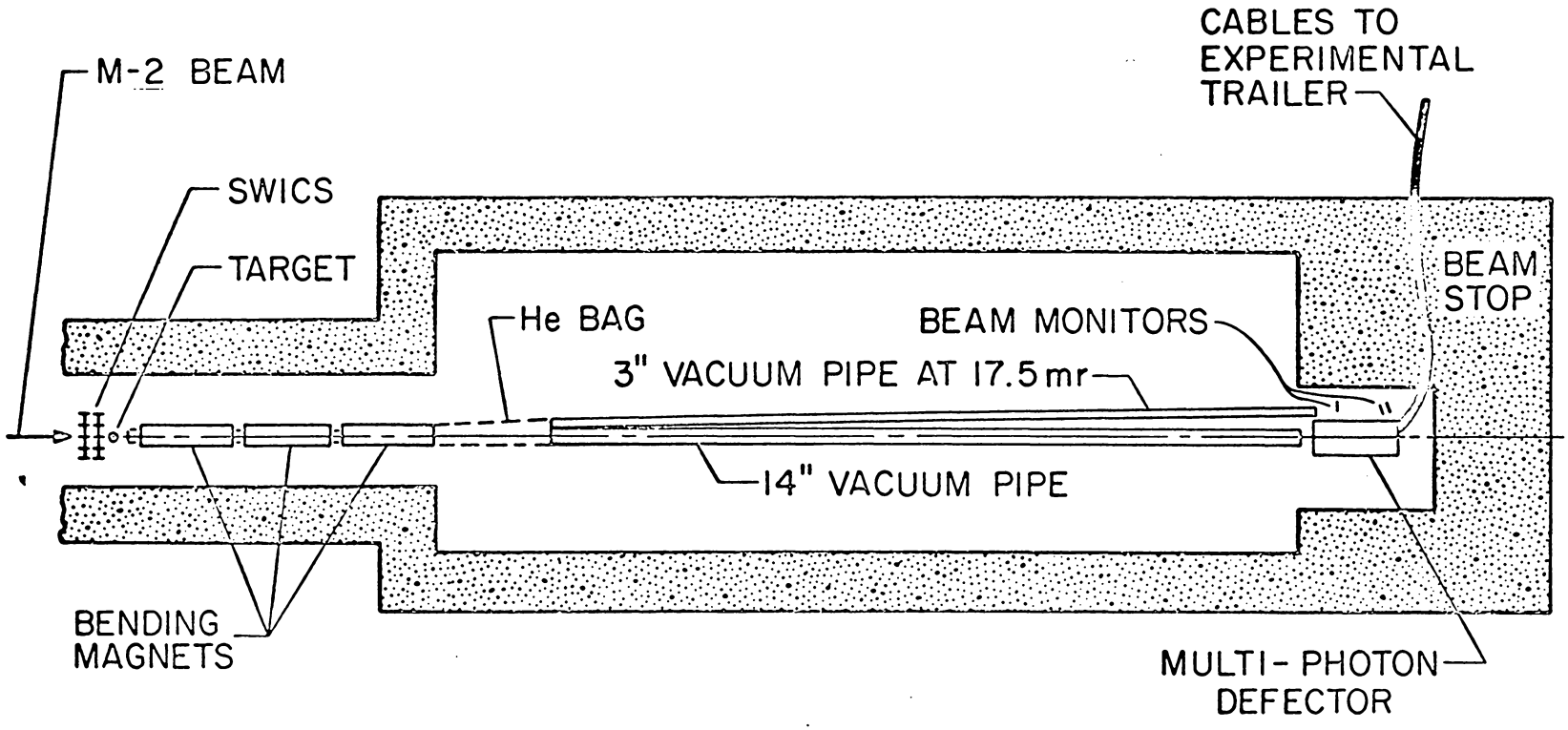

Figure 2. Schematic of Experimental Set-Up.

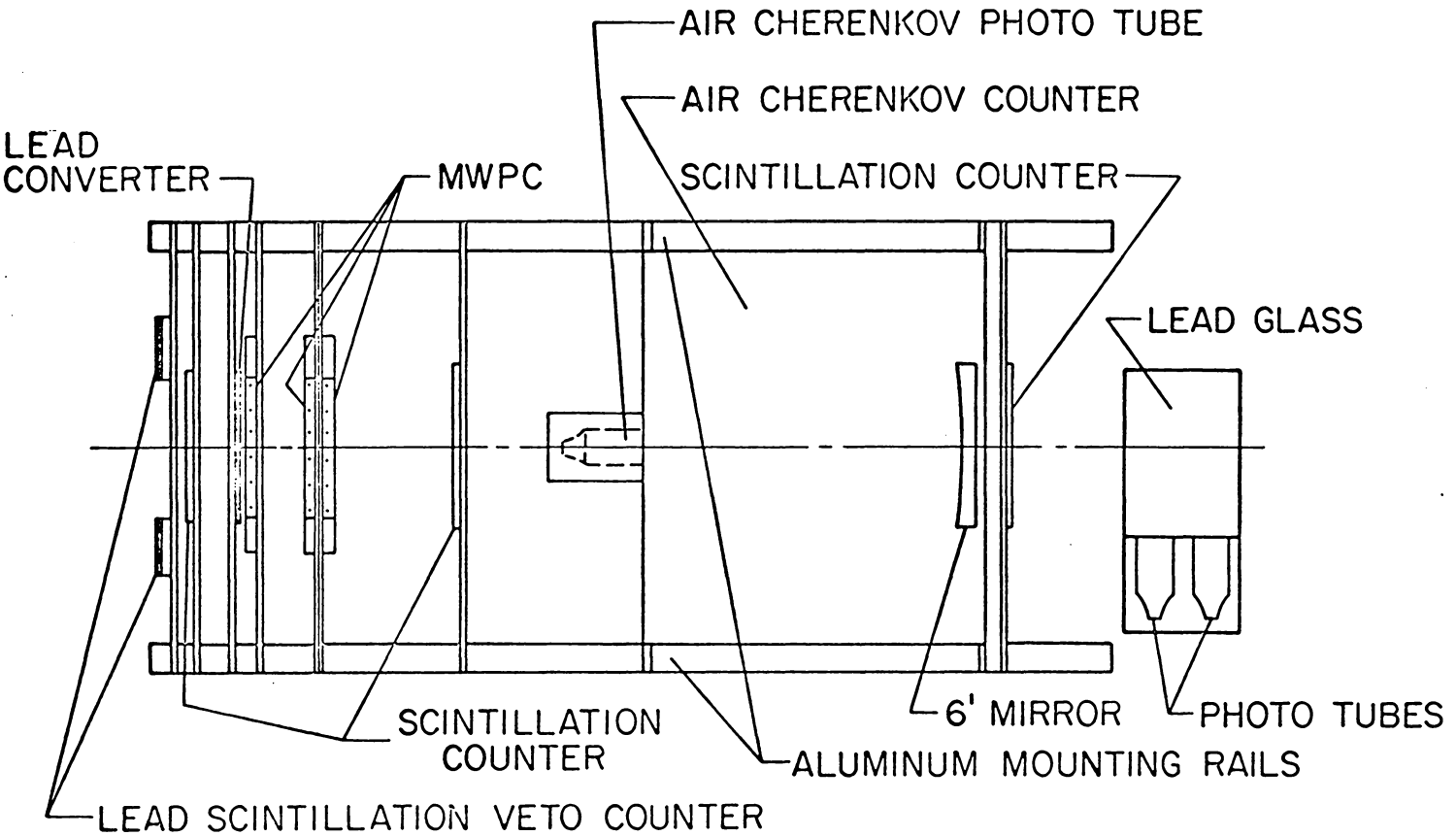

Figure 3. Schematic of Multi-Photon Detector.

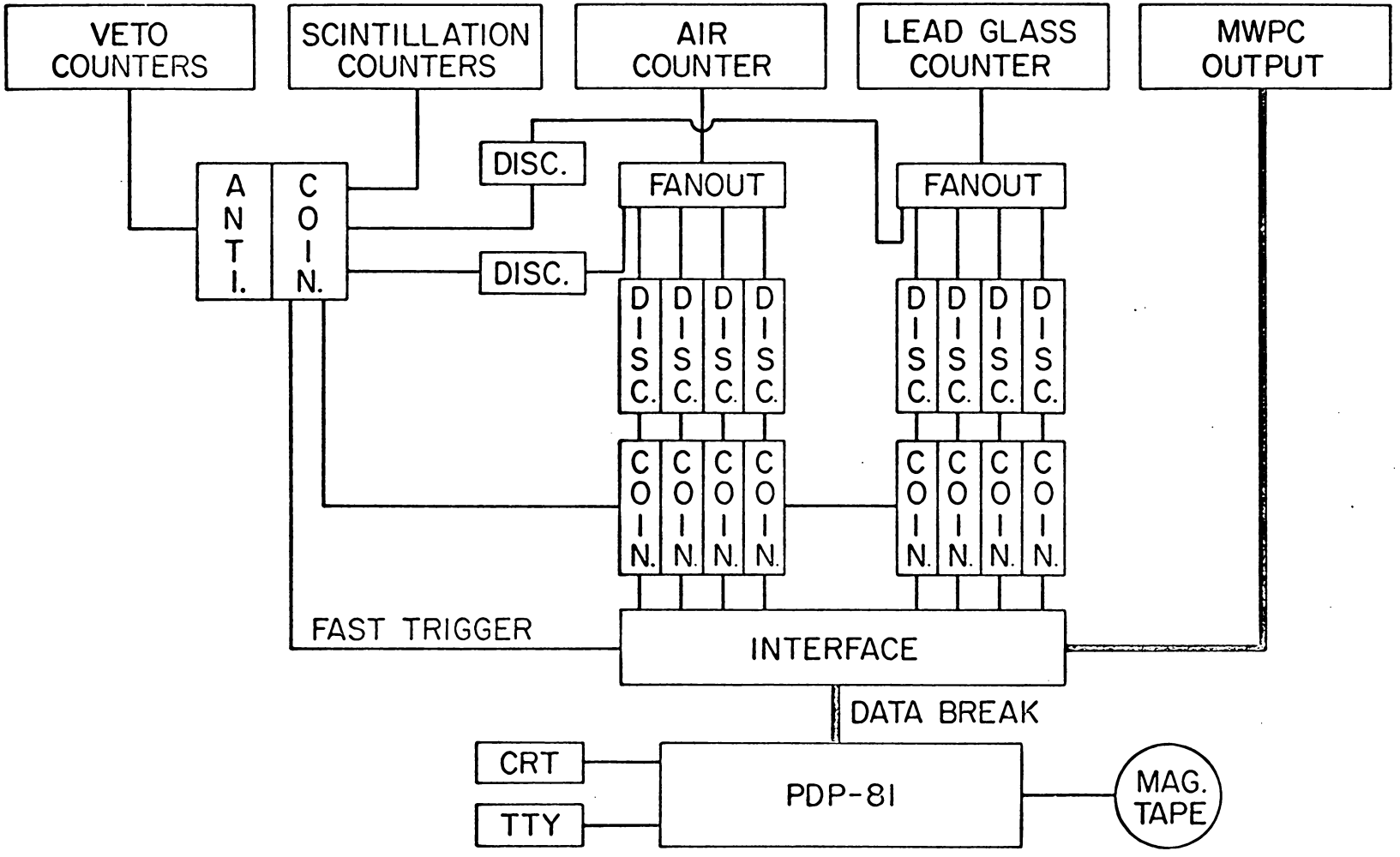

Figure 4. Schematic of Fast Trigger Logic.

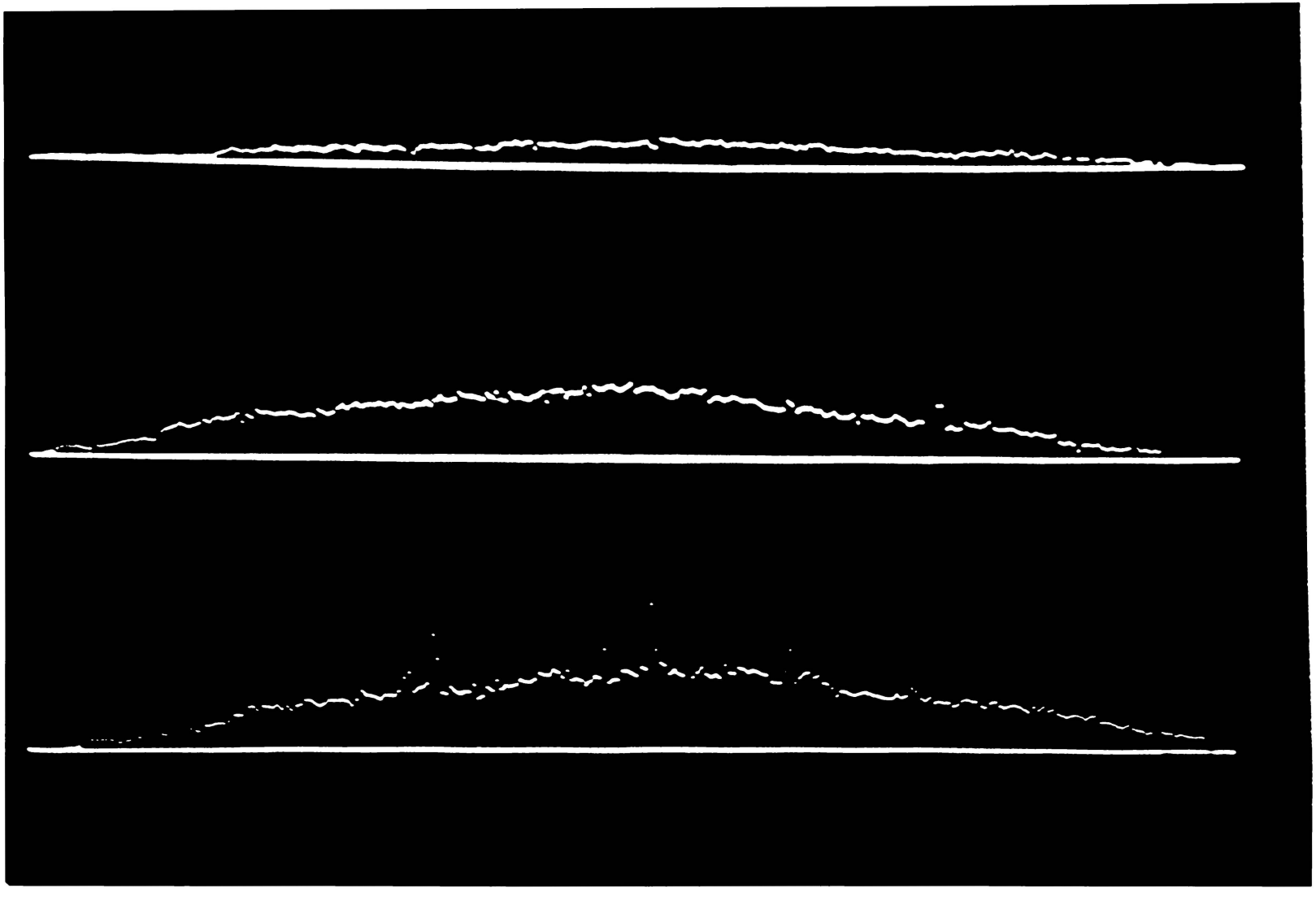

Figure 5. Scope Display of Proportional Chamber Wire Map.

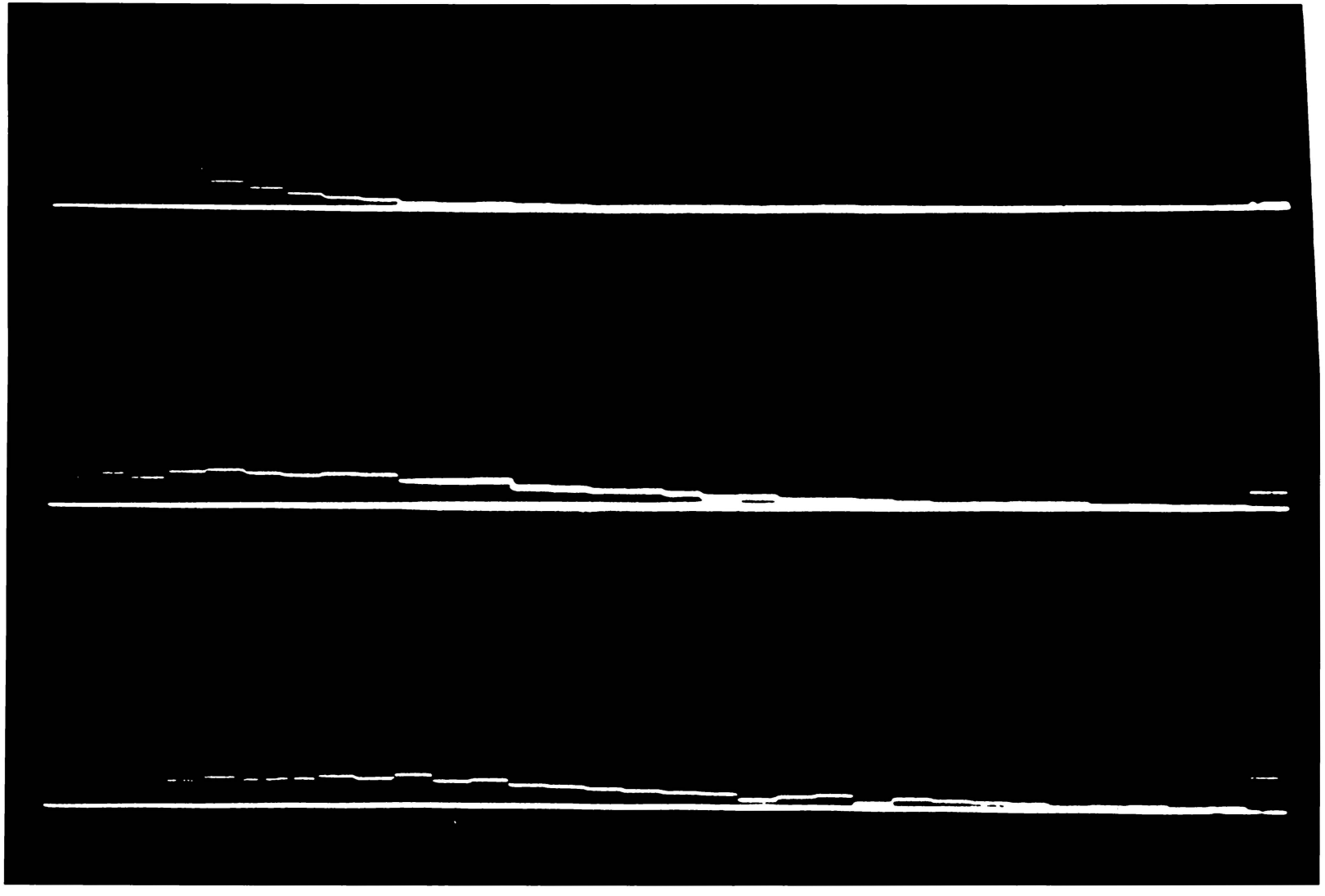

Figure 6. Scope Display of Multiplicity Distribution.

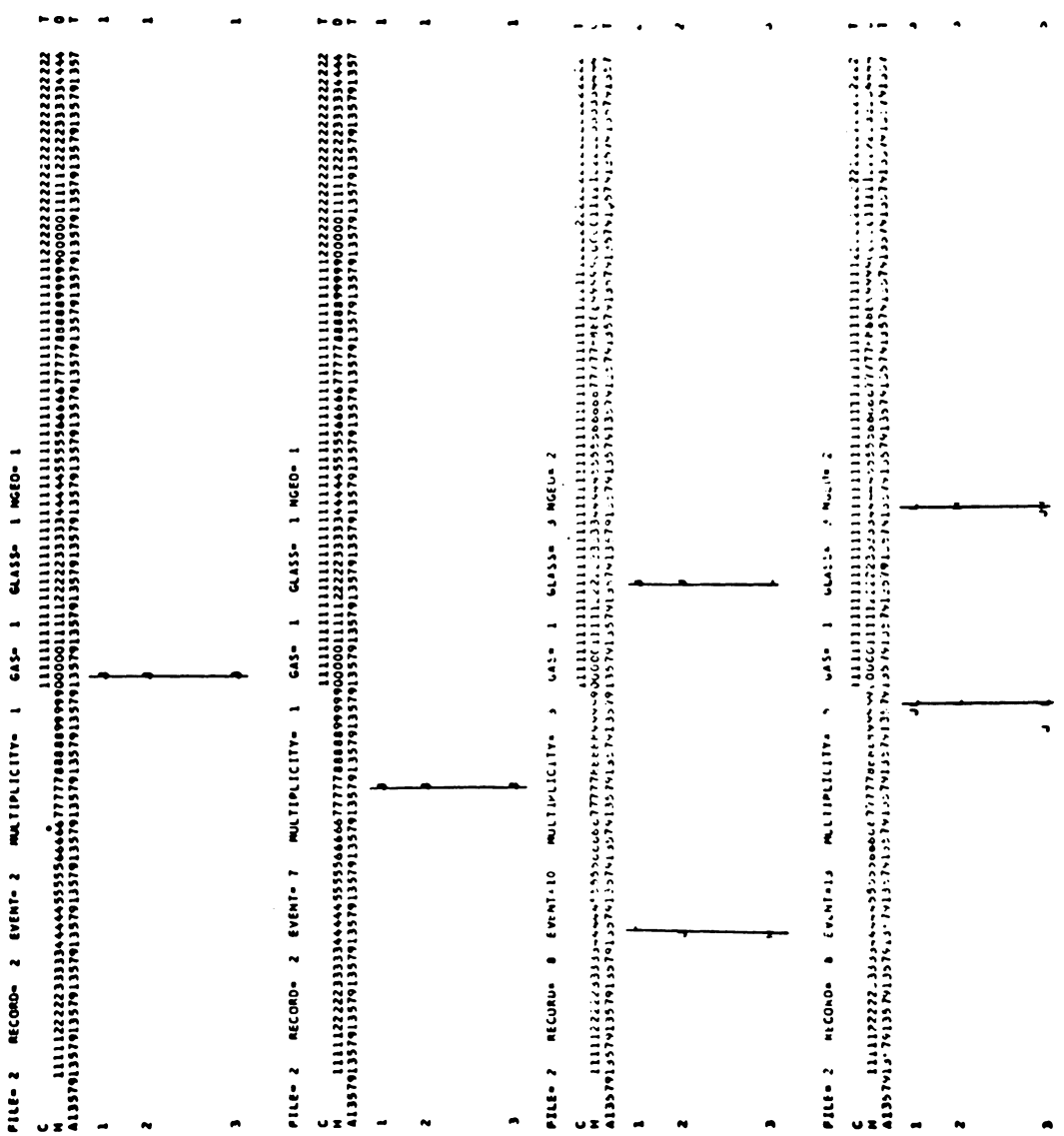

Figure 7. Typical Events with 1 or 2 Particles.

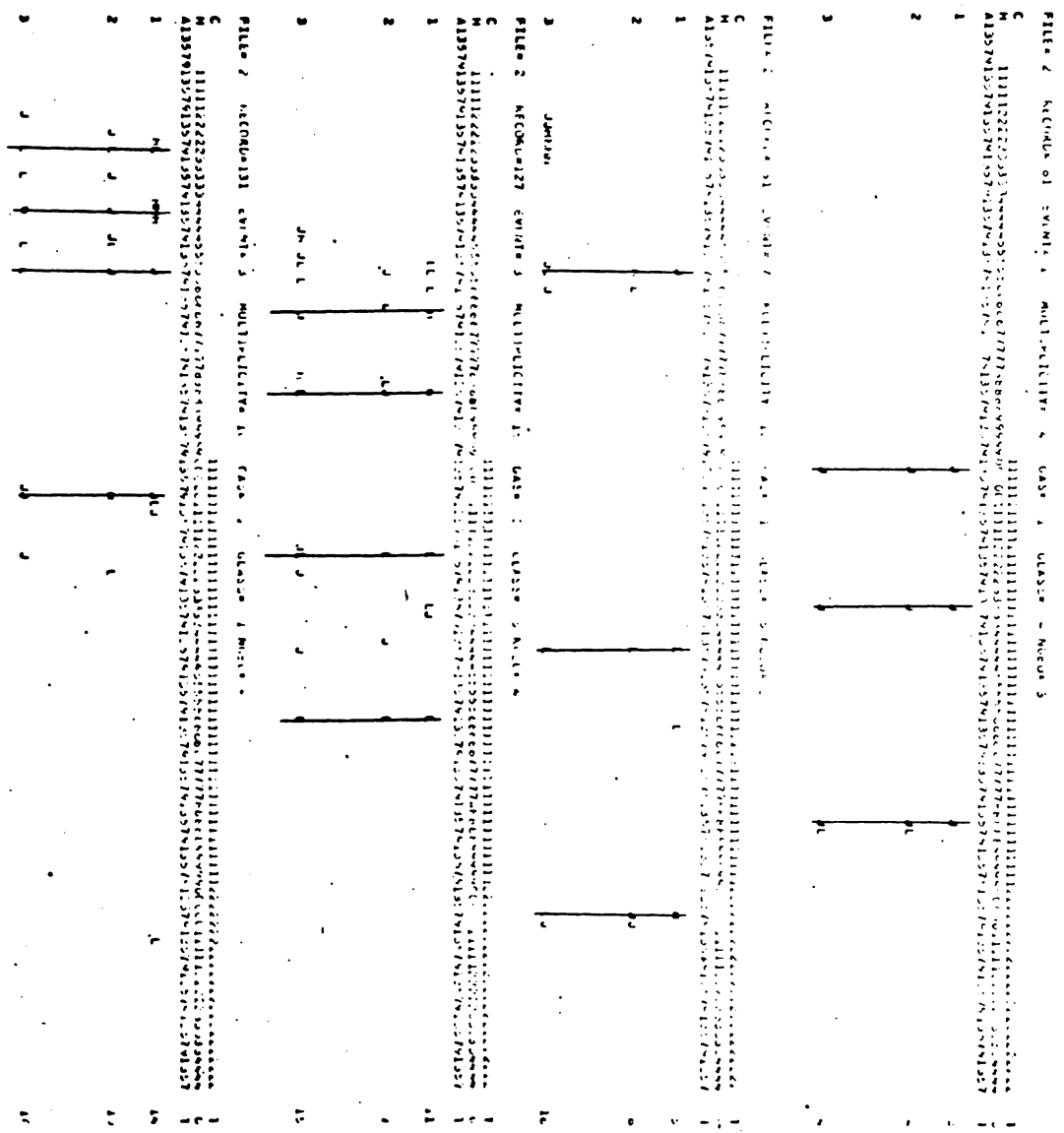

Figure 8. Typical Events with 3 or 4 Particles.

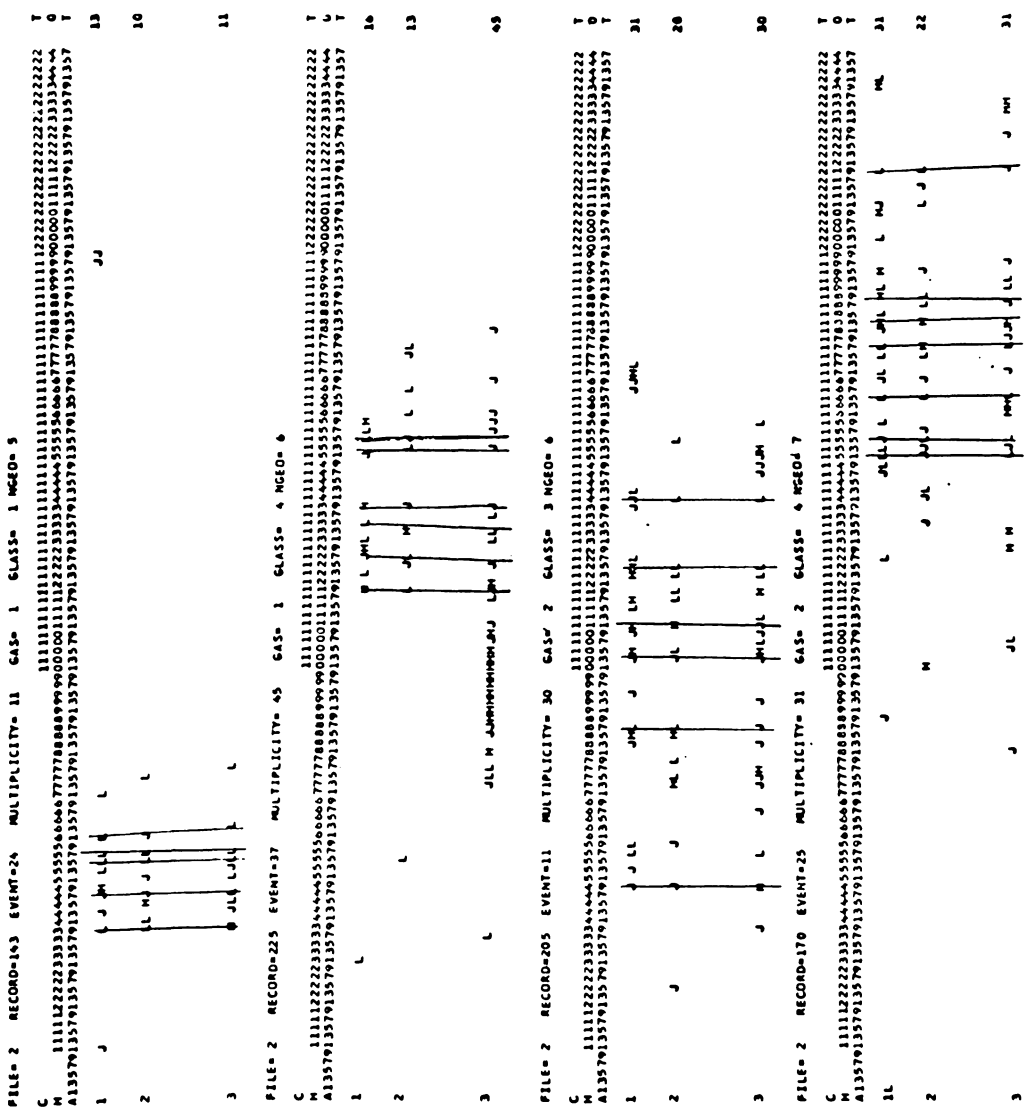

Figure 9. Typical Events with 5 or more Particles.

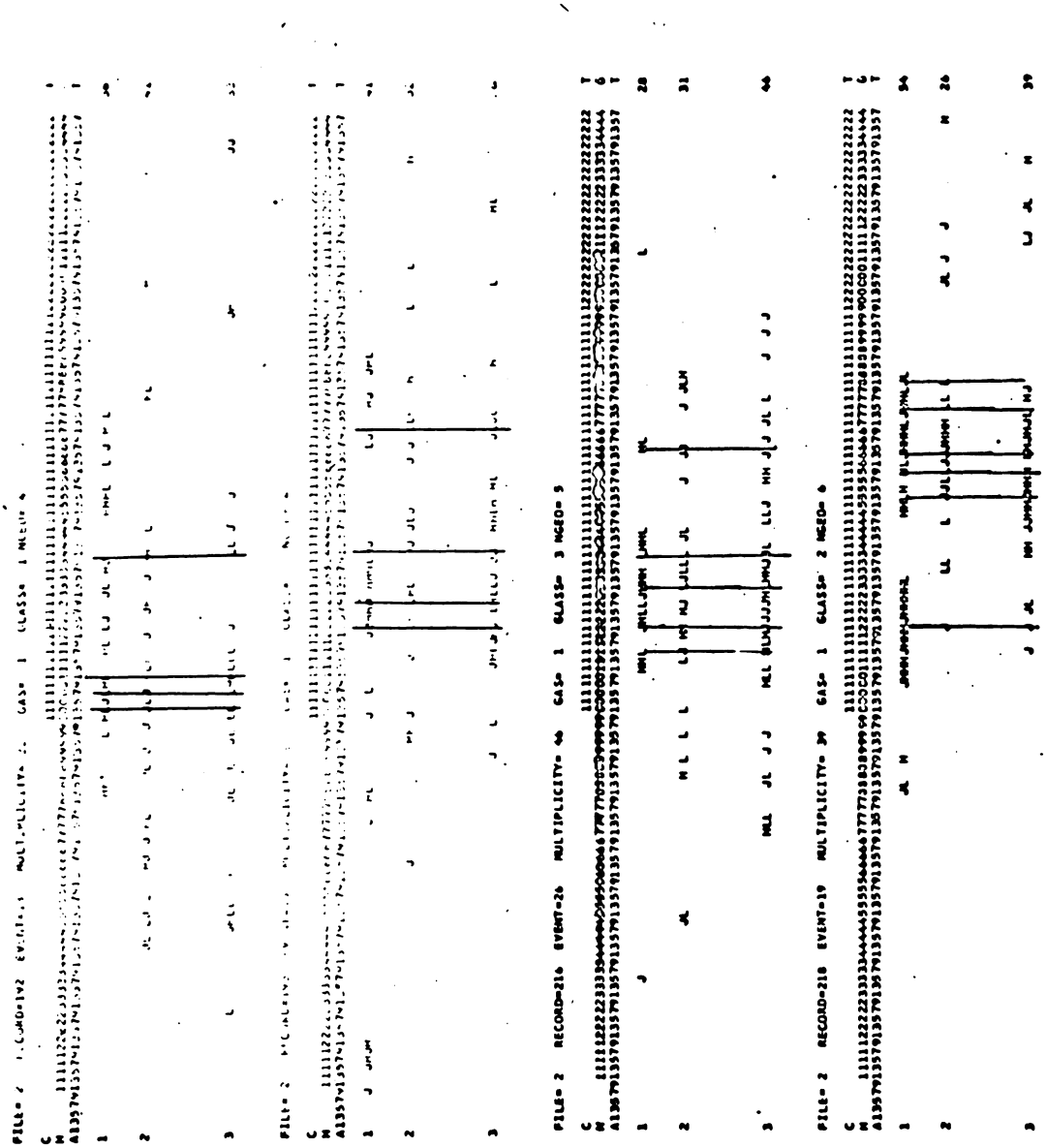

Figure 10. Events with Questionable Multiplicity.

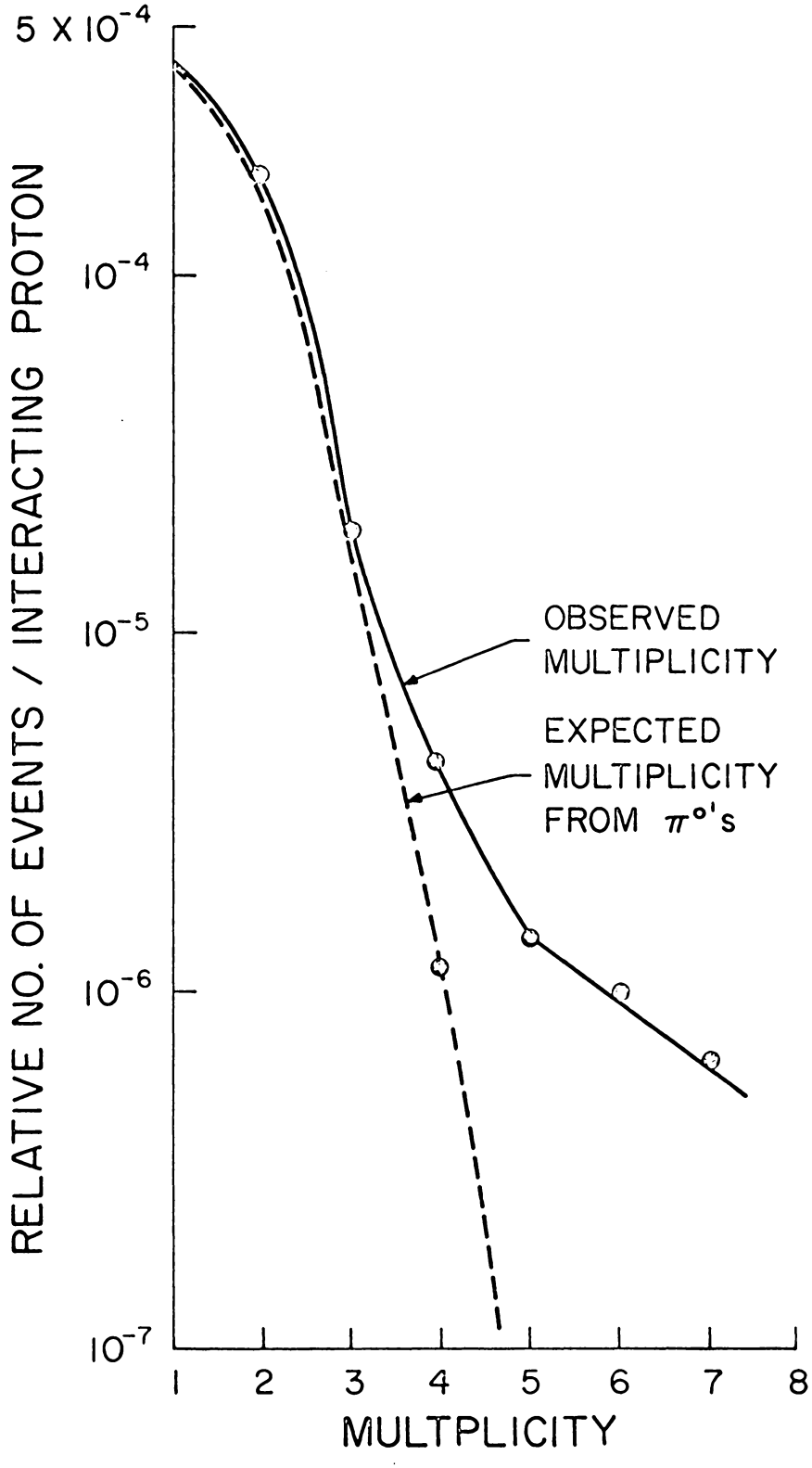

Figure 11. Multiplicity Distribution of Events.

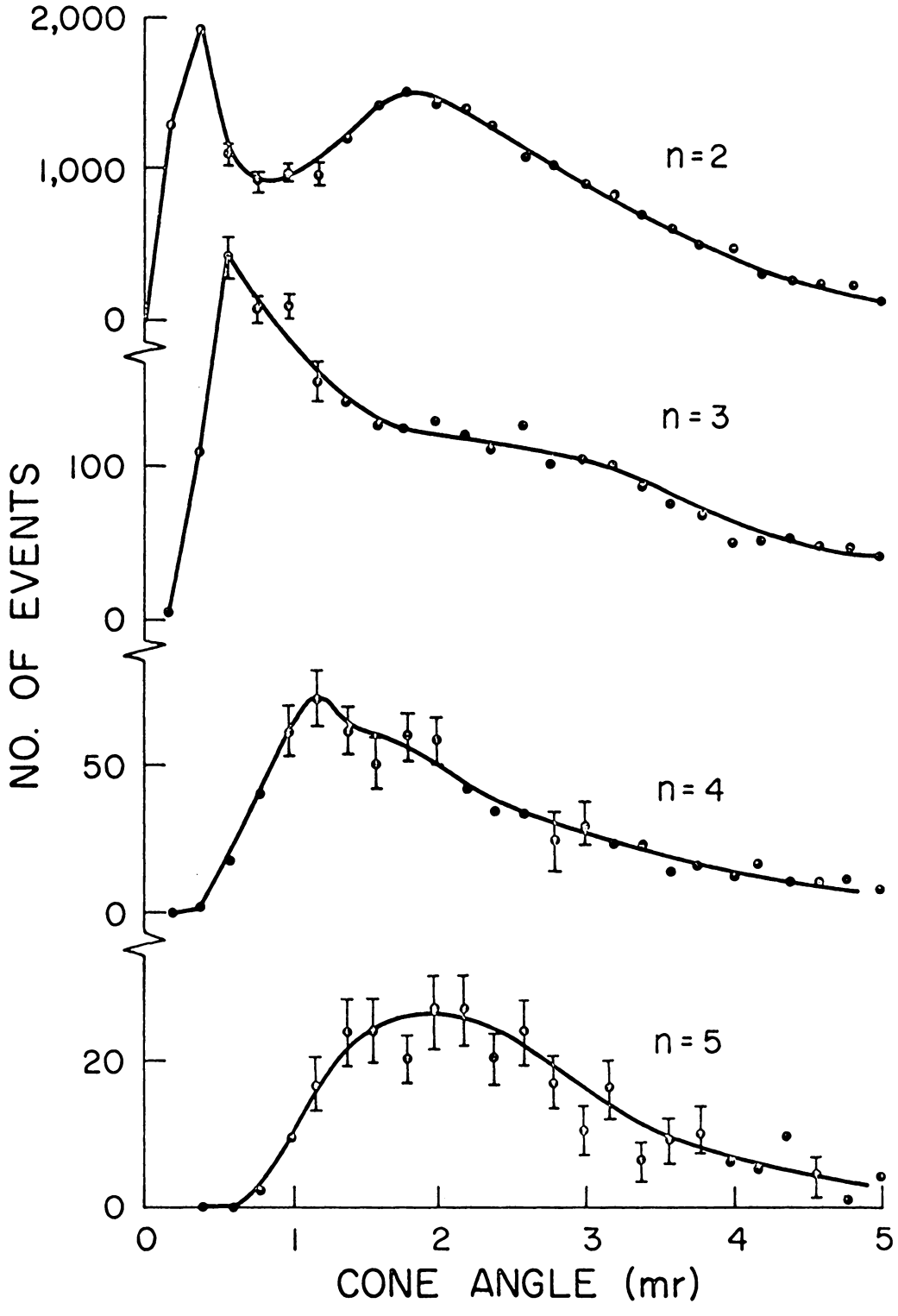

Figure 12. Projected Cone Angle of Events.

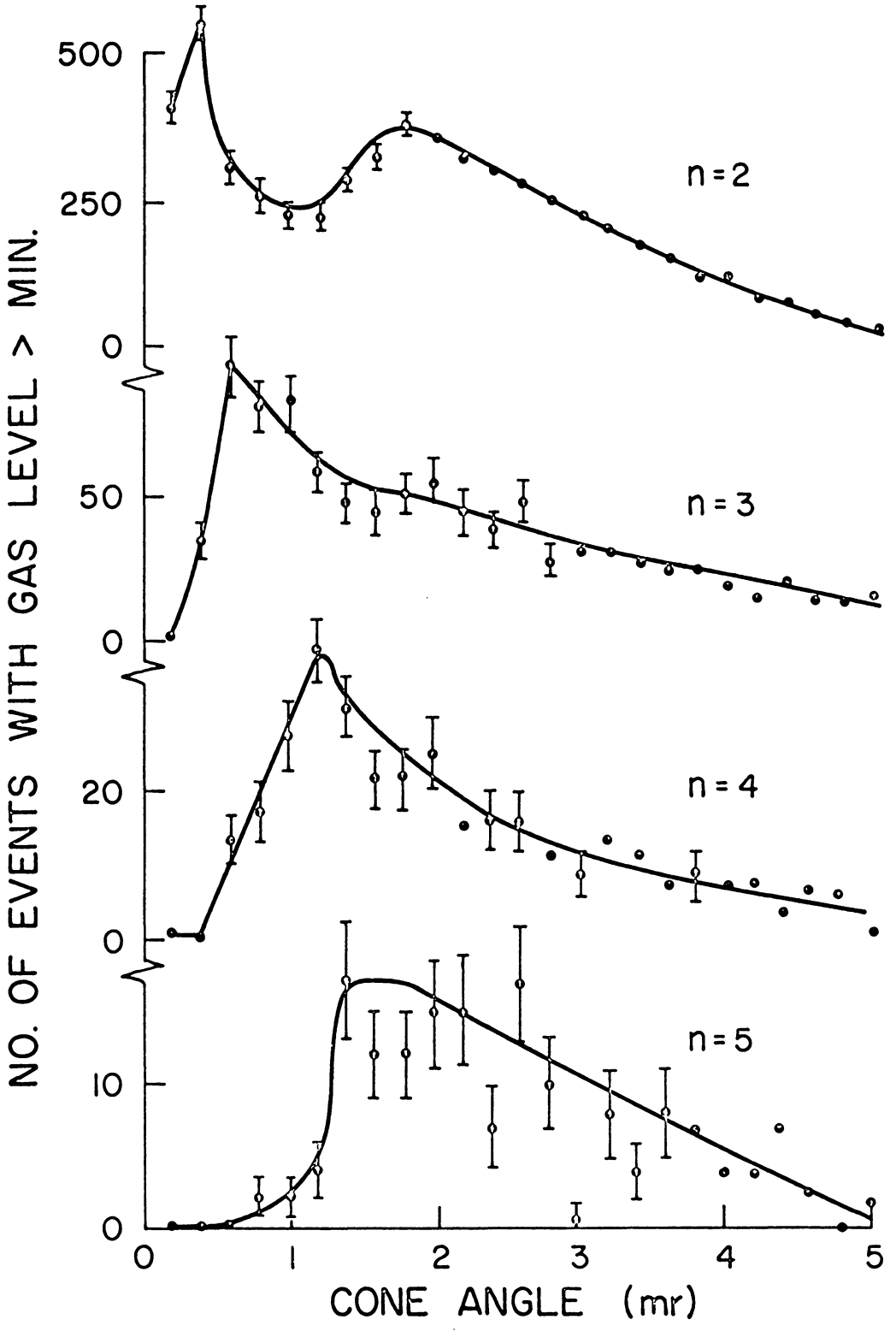

Figure 13. Projected Cone Angle of Events with Gas Levels > Minimum.

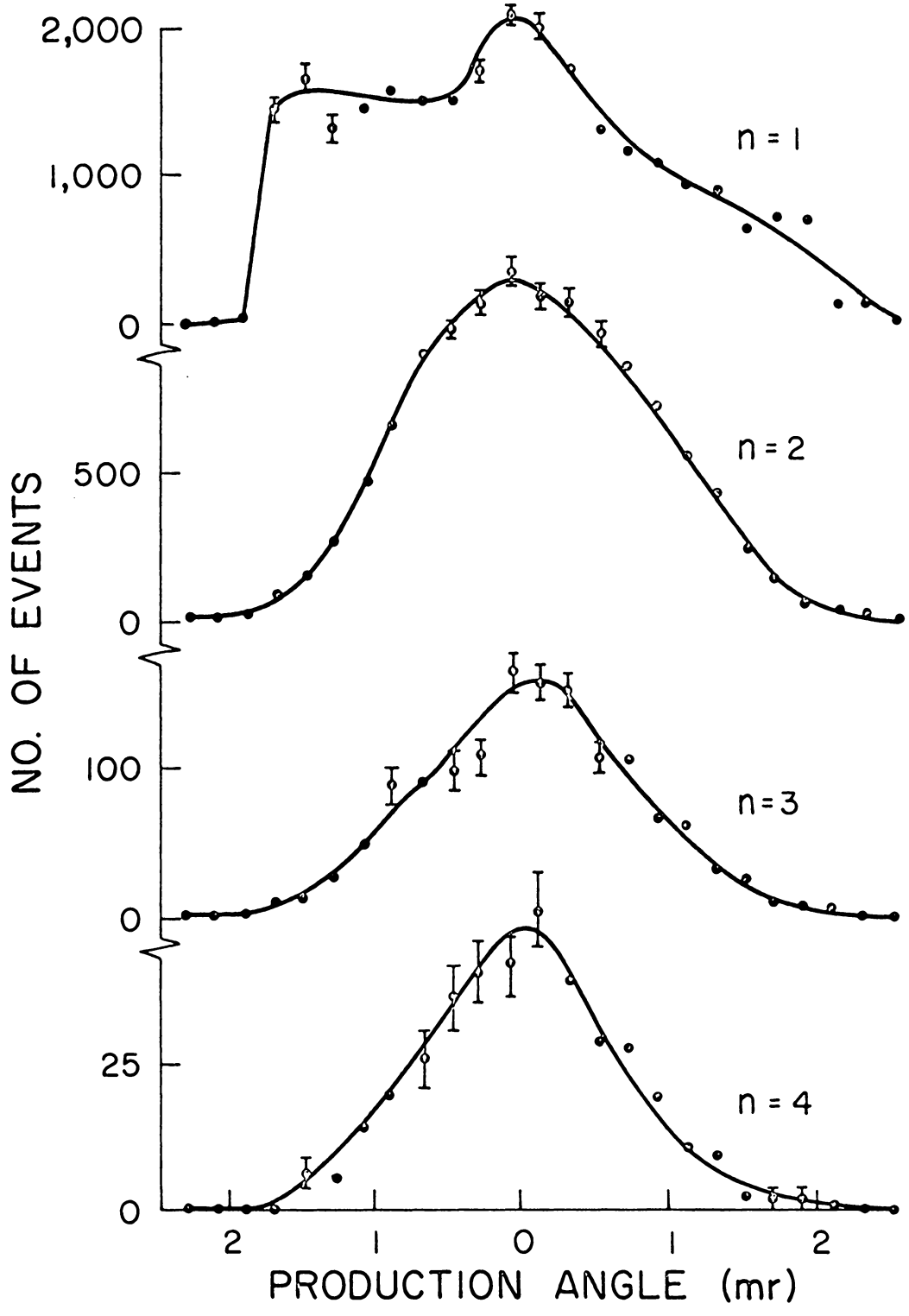

Figure 14. Production Angle of Events.

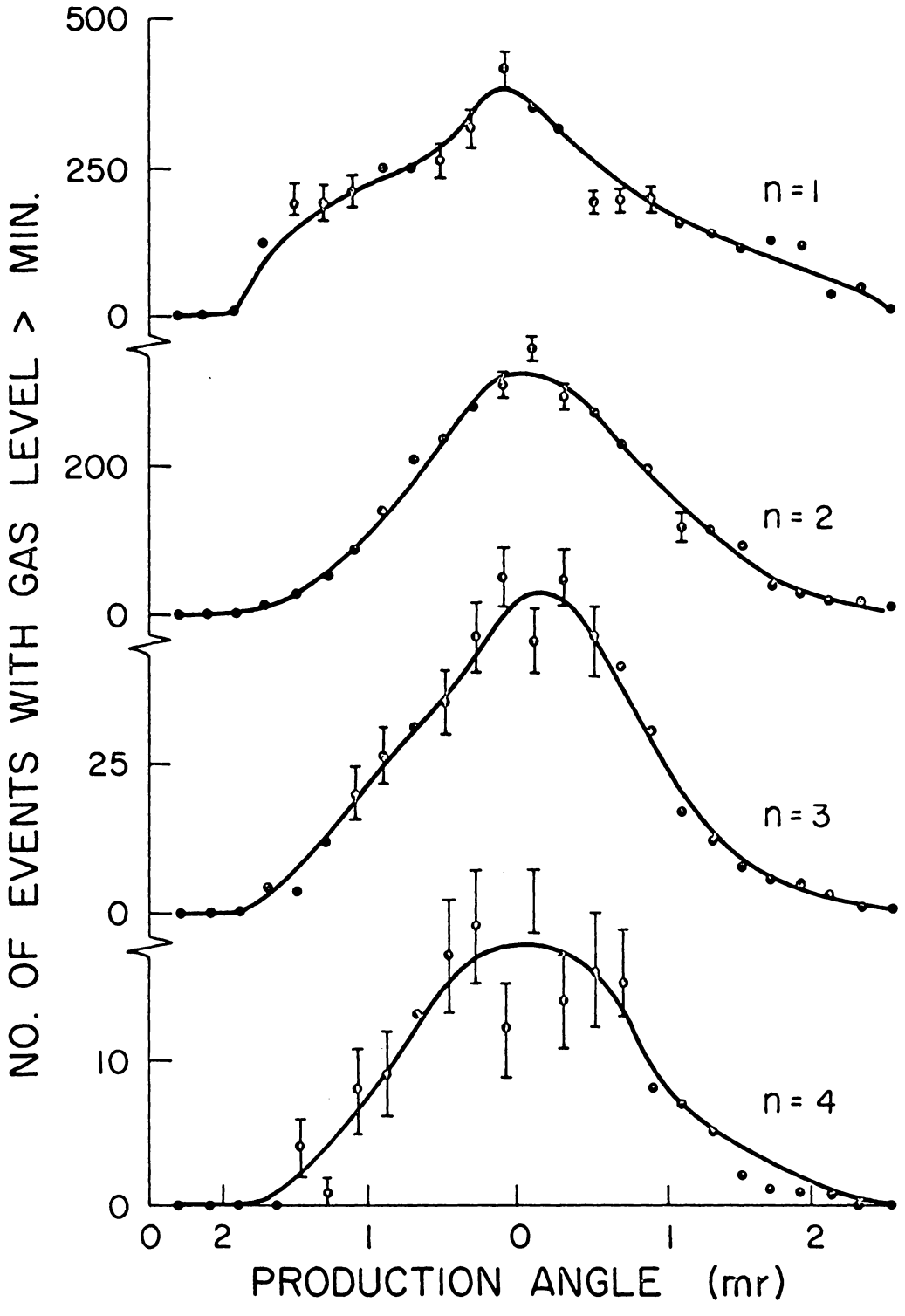

Figure 15. Production Angle of Events with Gas Levels > Minimum.

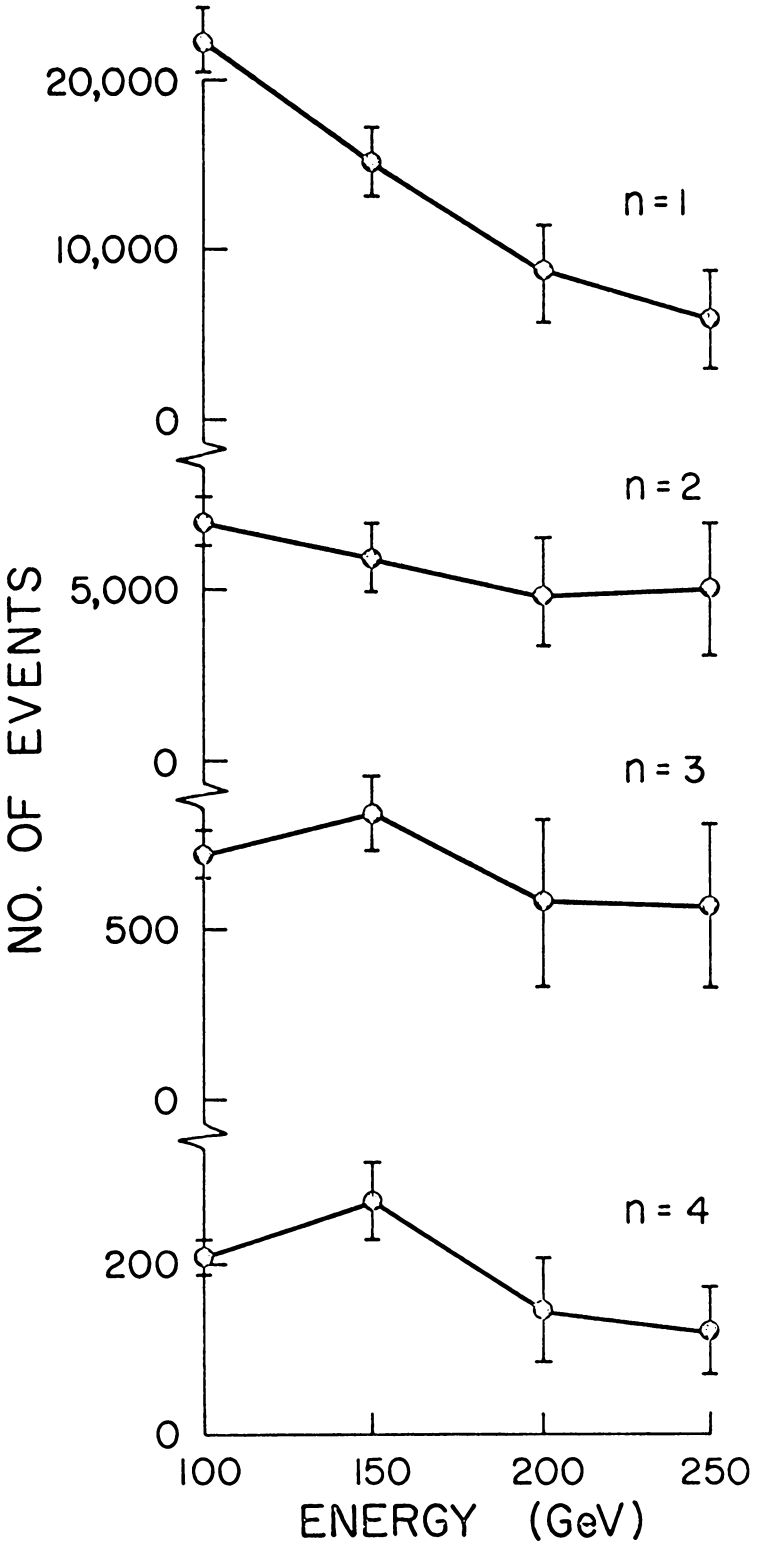

Figure 16. Energy Distribution of Events.

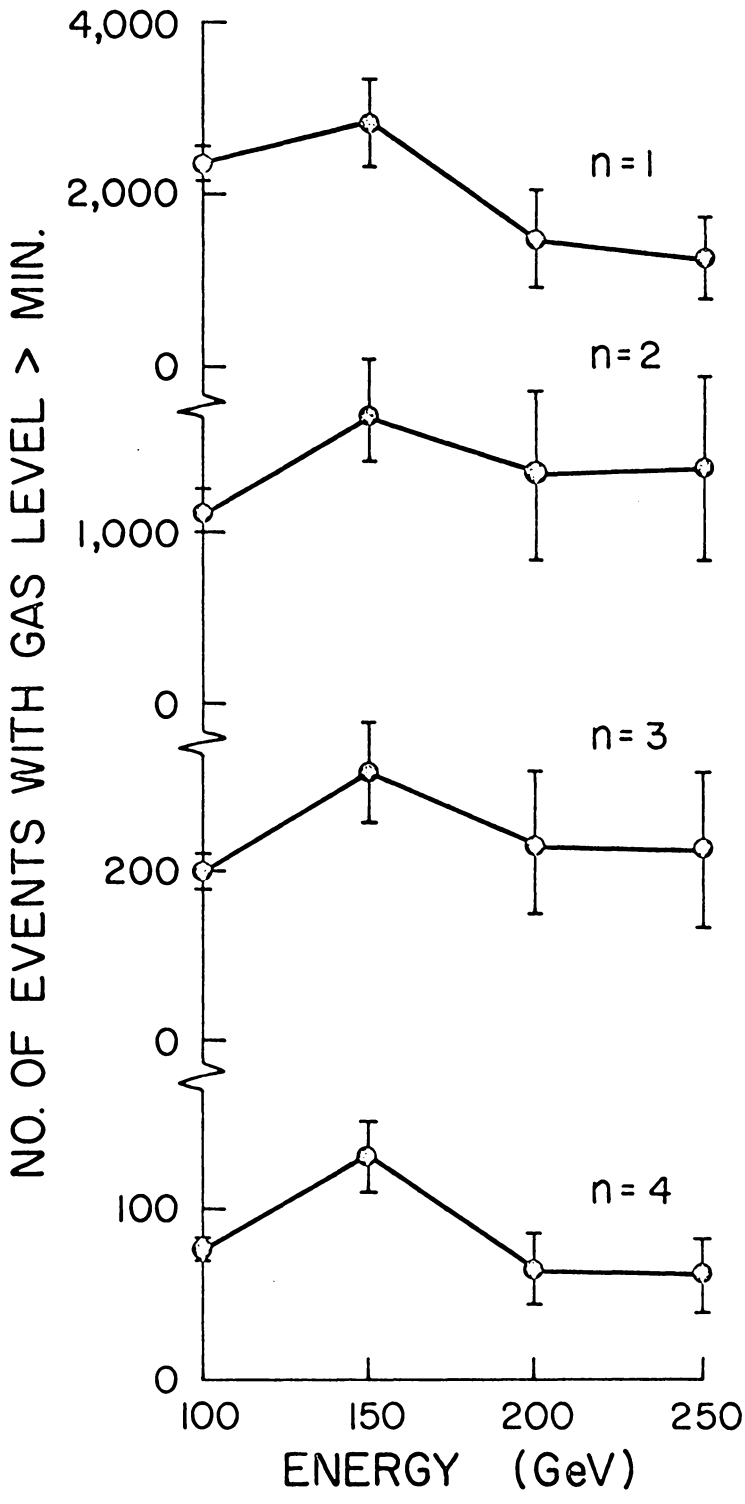

Figure 17. Energy Distribution of Events with Gas Levels > Minimum.

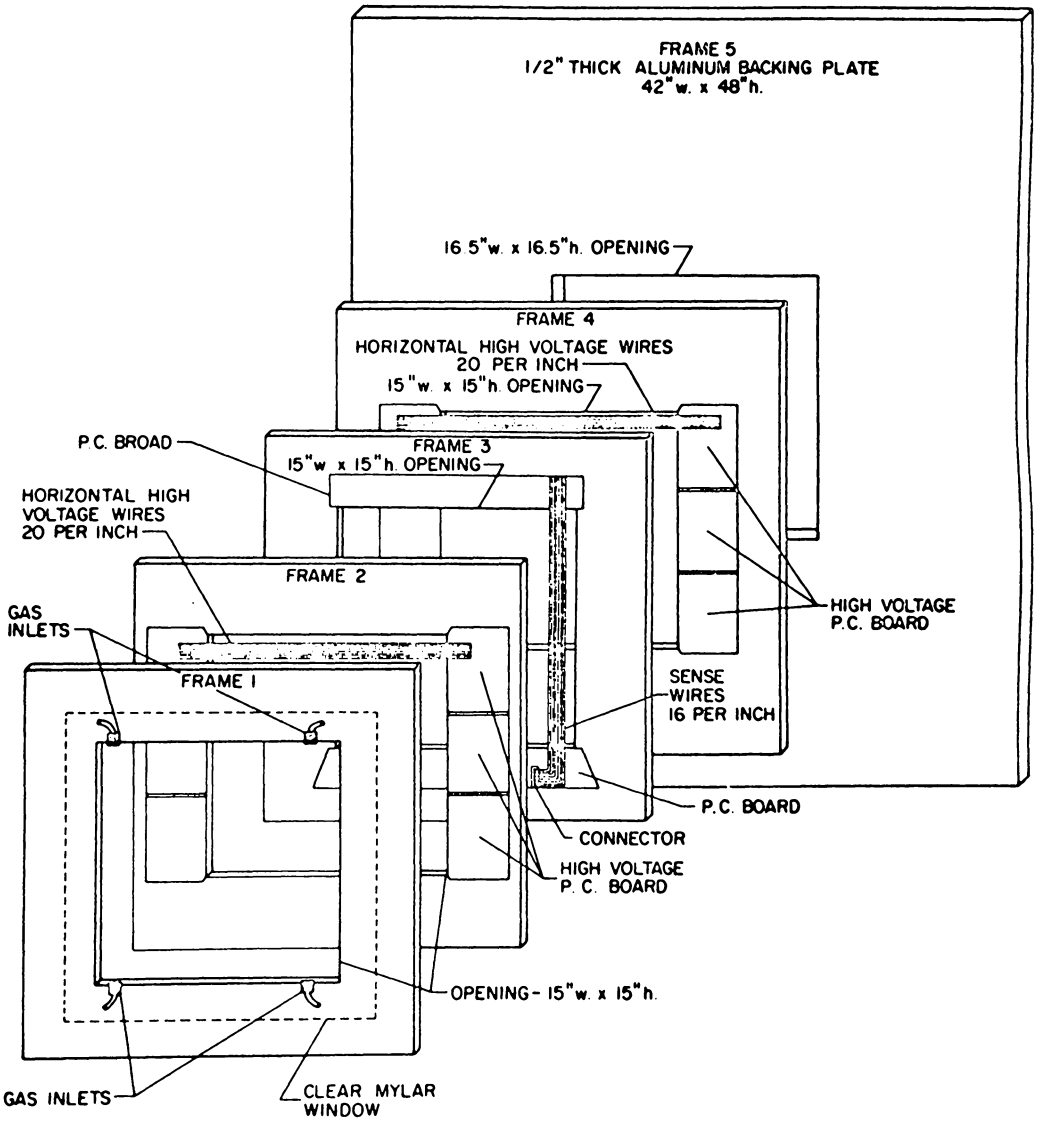

Figure 18. Schematic of Multi-Wire Proportional Chamber.

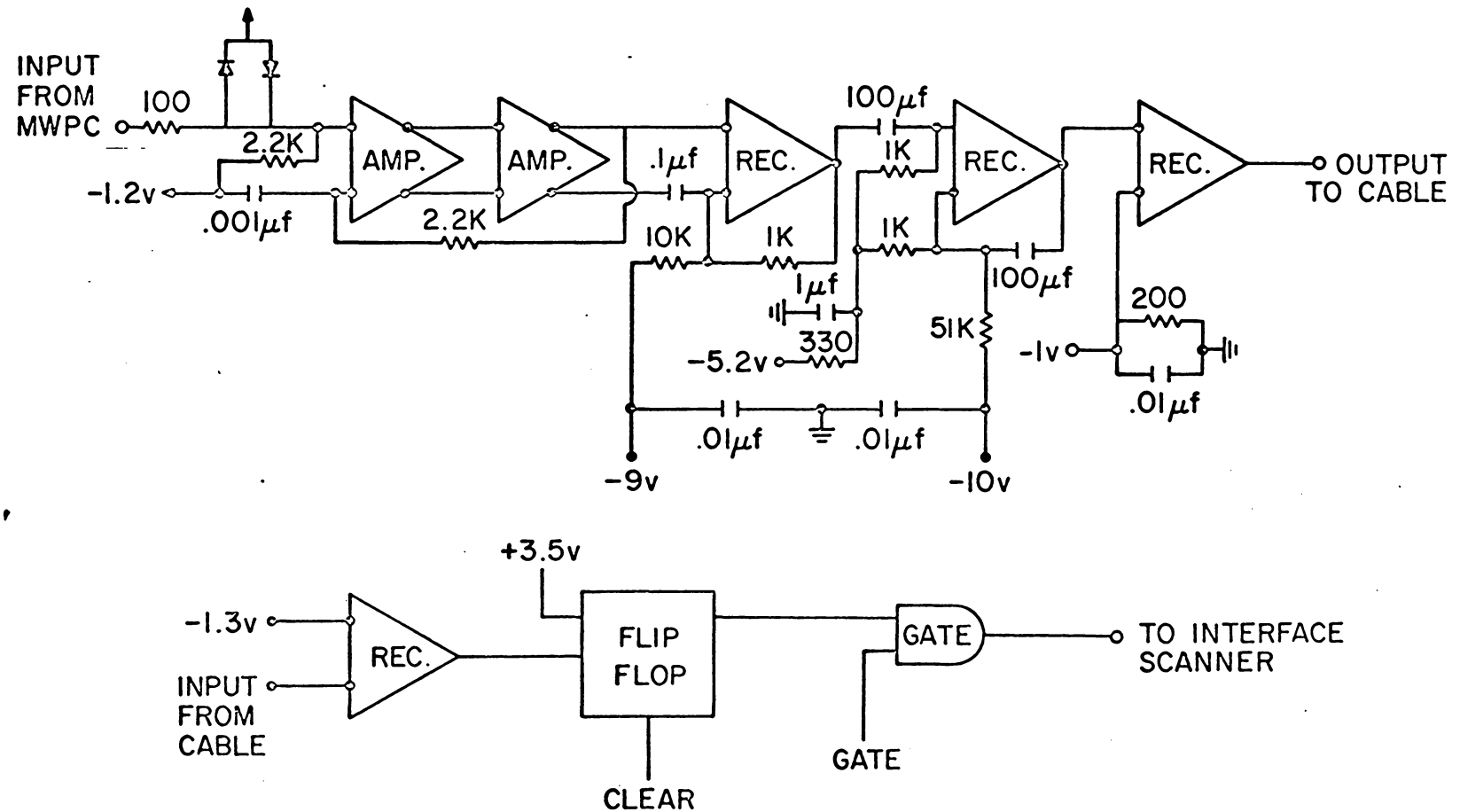

Figure 19. Transmitter Card and Receiver Card Logic.

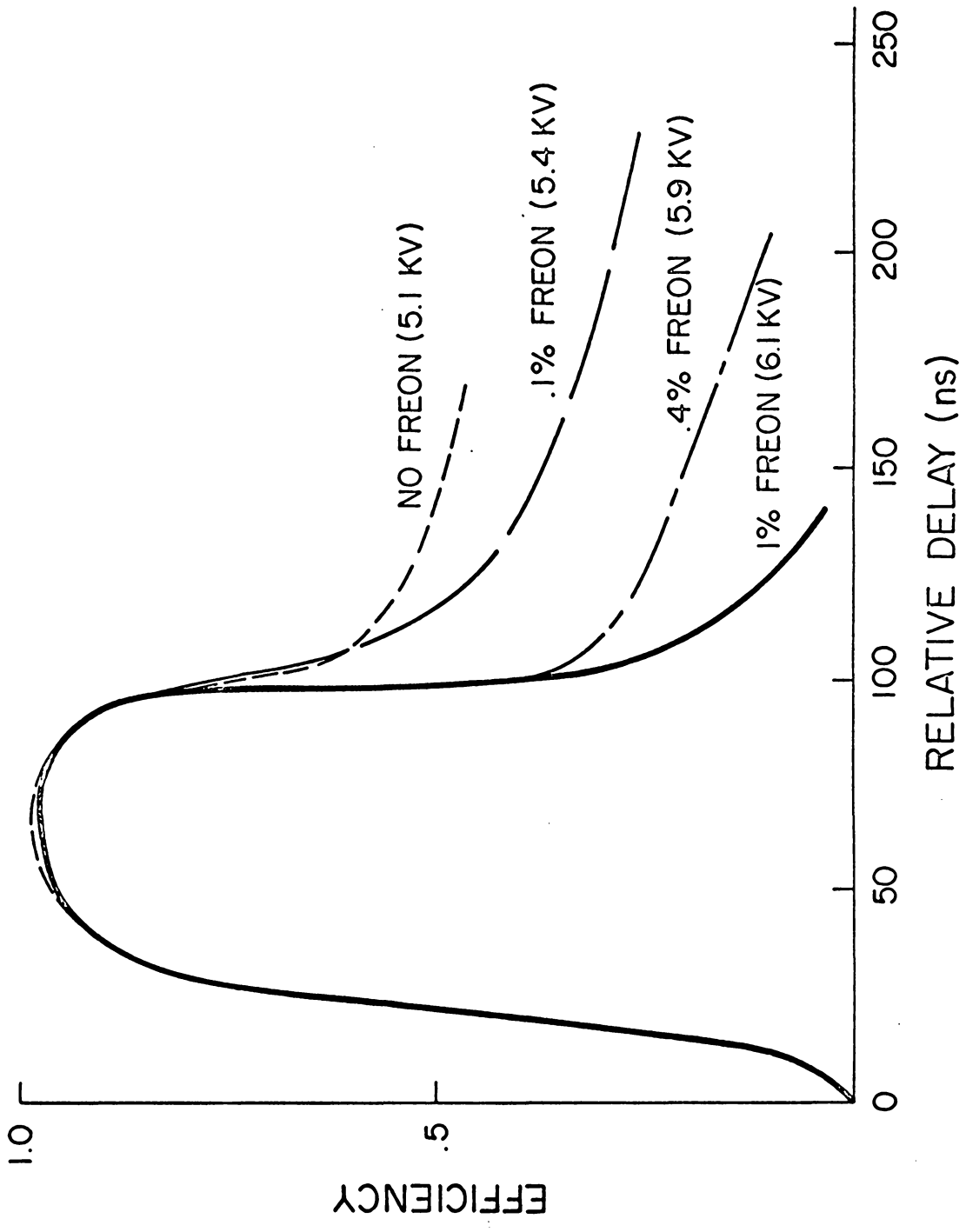

Figure 20. Chamber Efficiency as a Function of Delay.

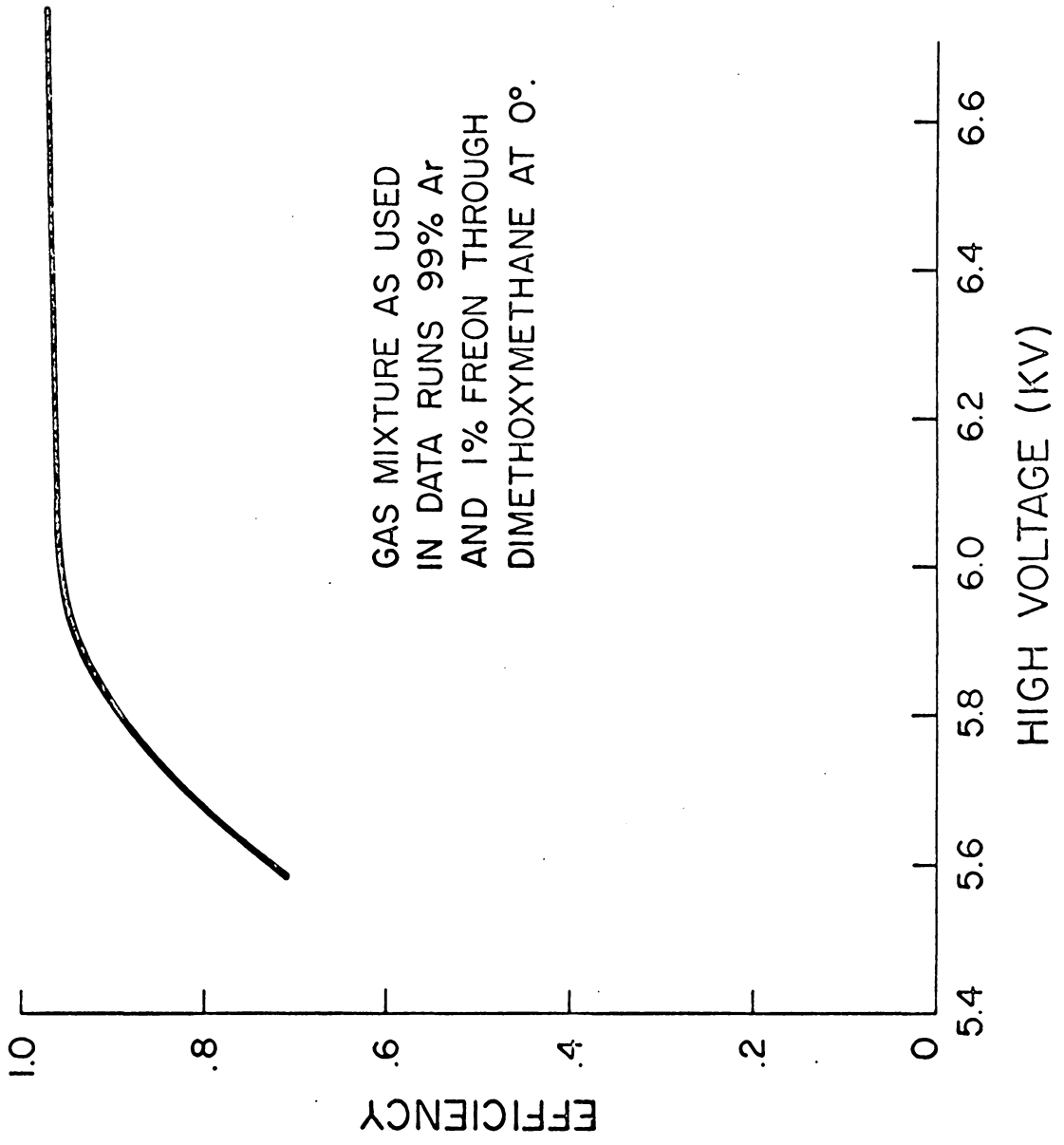

Figure 21. Chamber Efficiency as a Function of High Voltage.

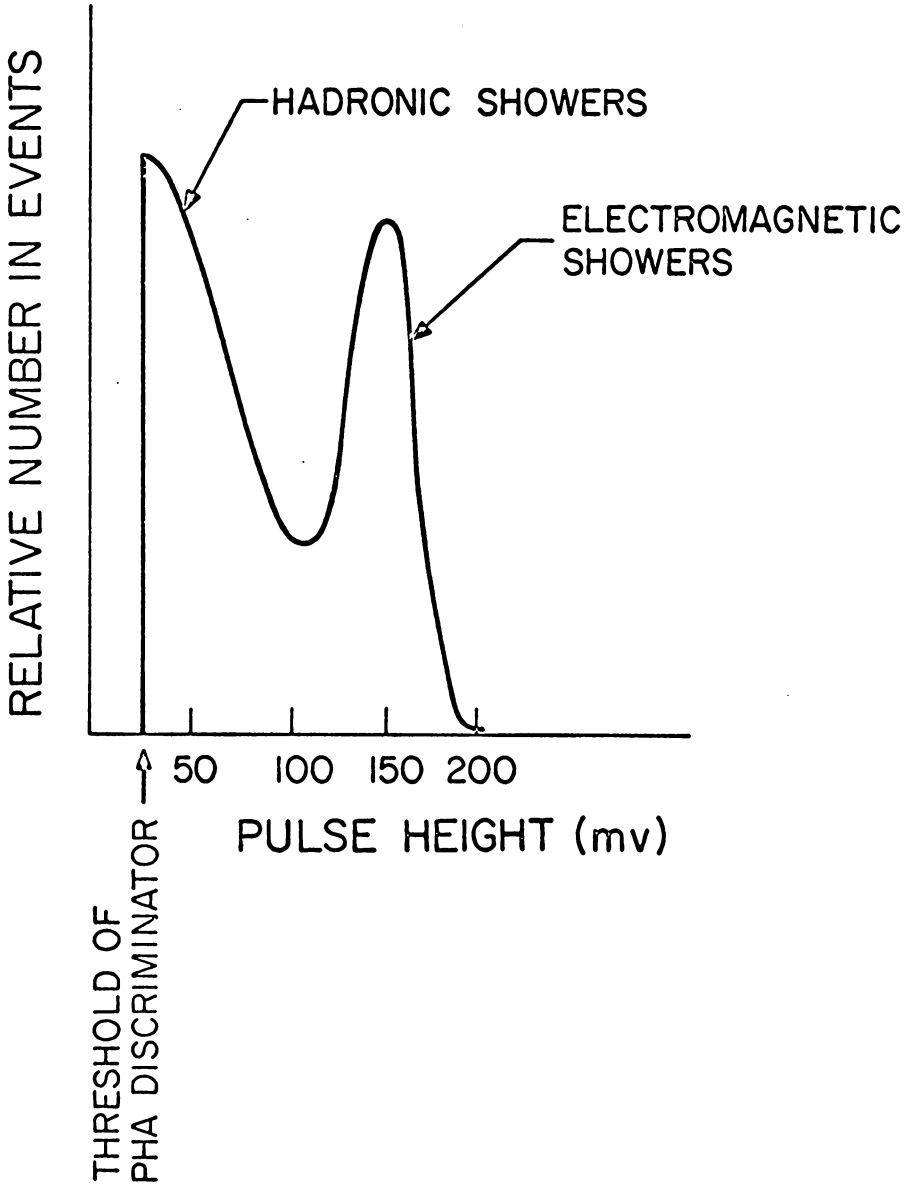

Figure 22. Lead Glass Counter Pulse Height for 40 GeV/c Particles.

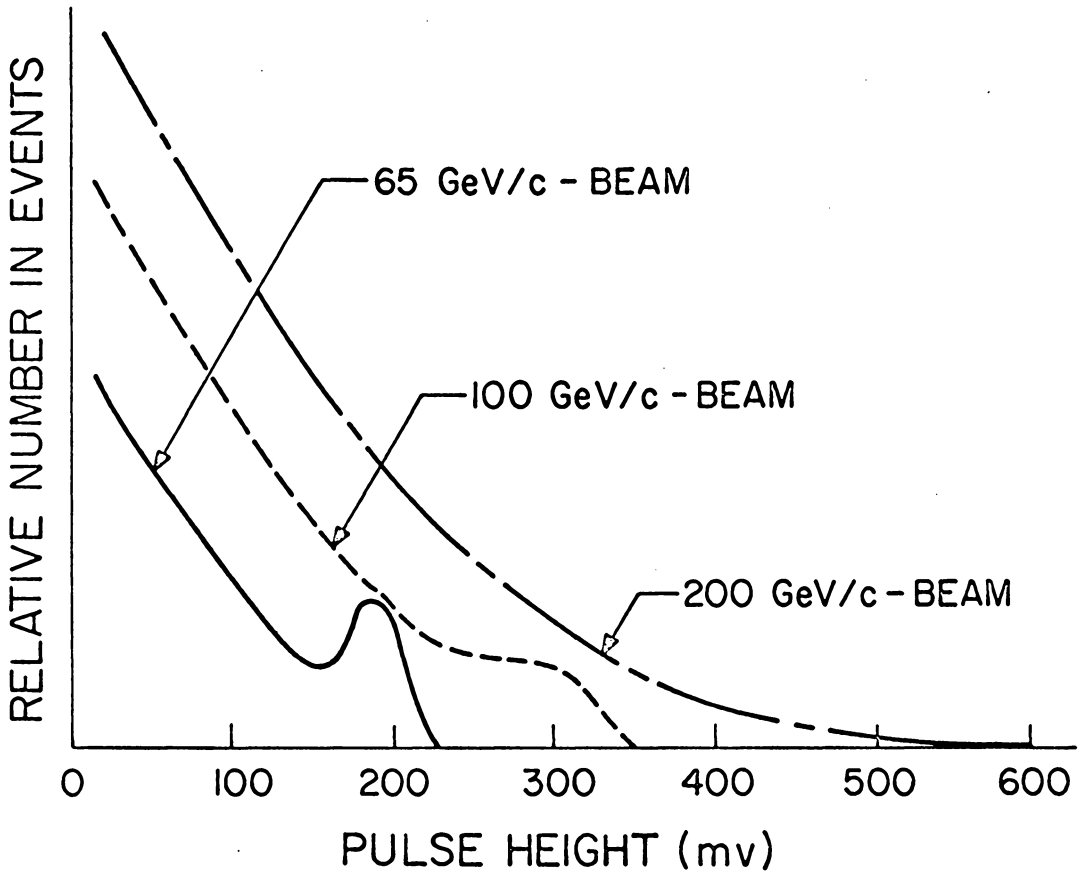

Figure 23. Pulse Height for 65, 100, and 200 GeV/c Particles.

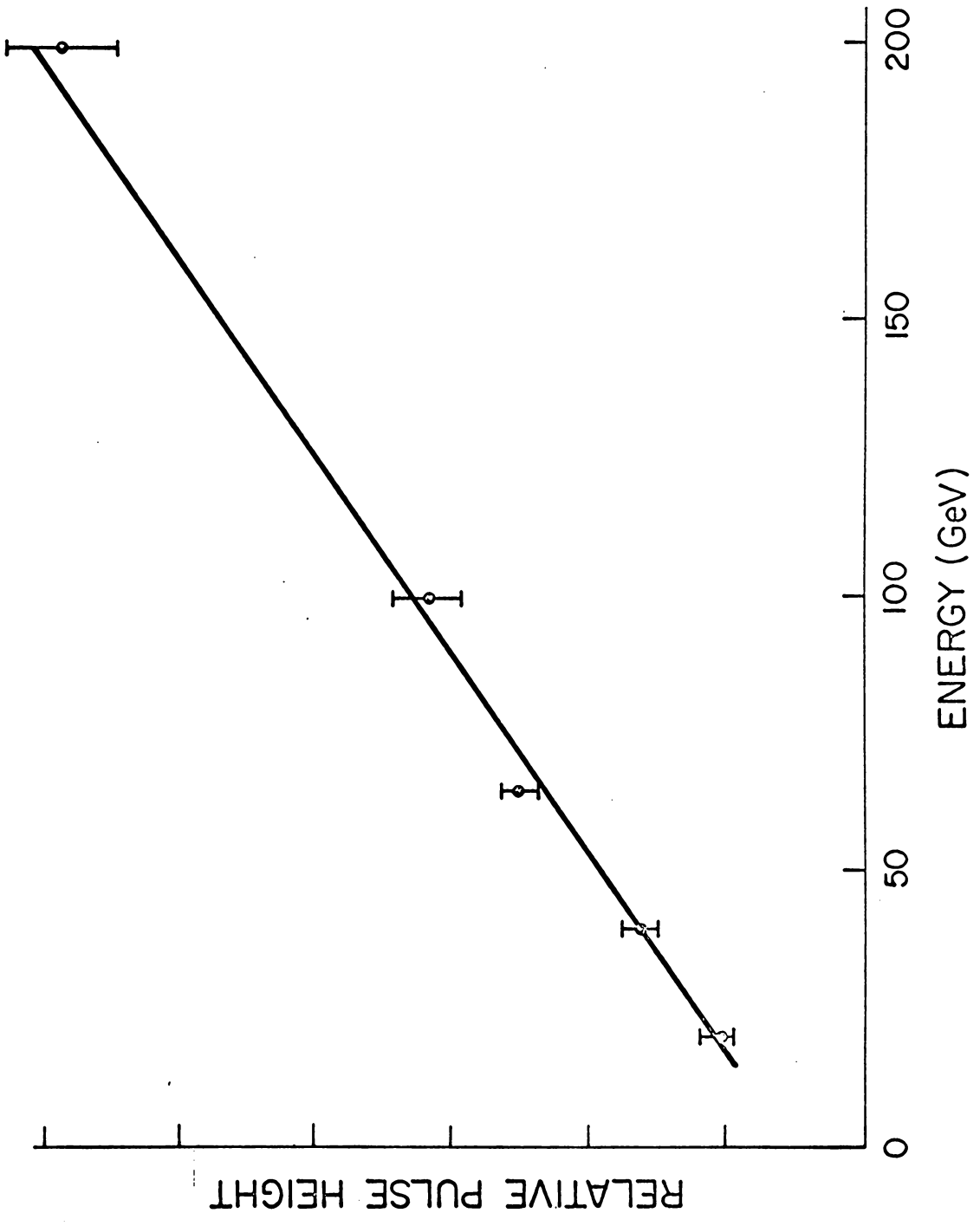

Figure 24. Response of Lead Glass as a Function of Electromagnetic Energy.

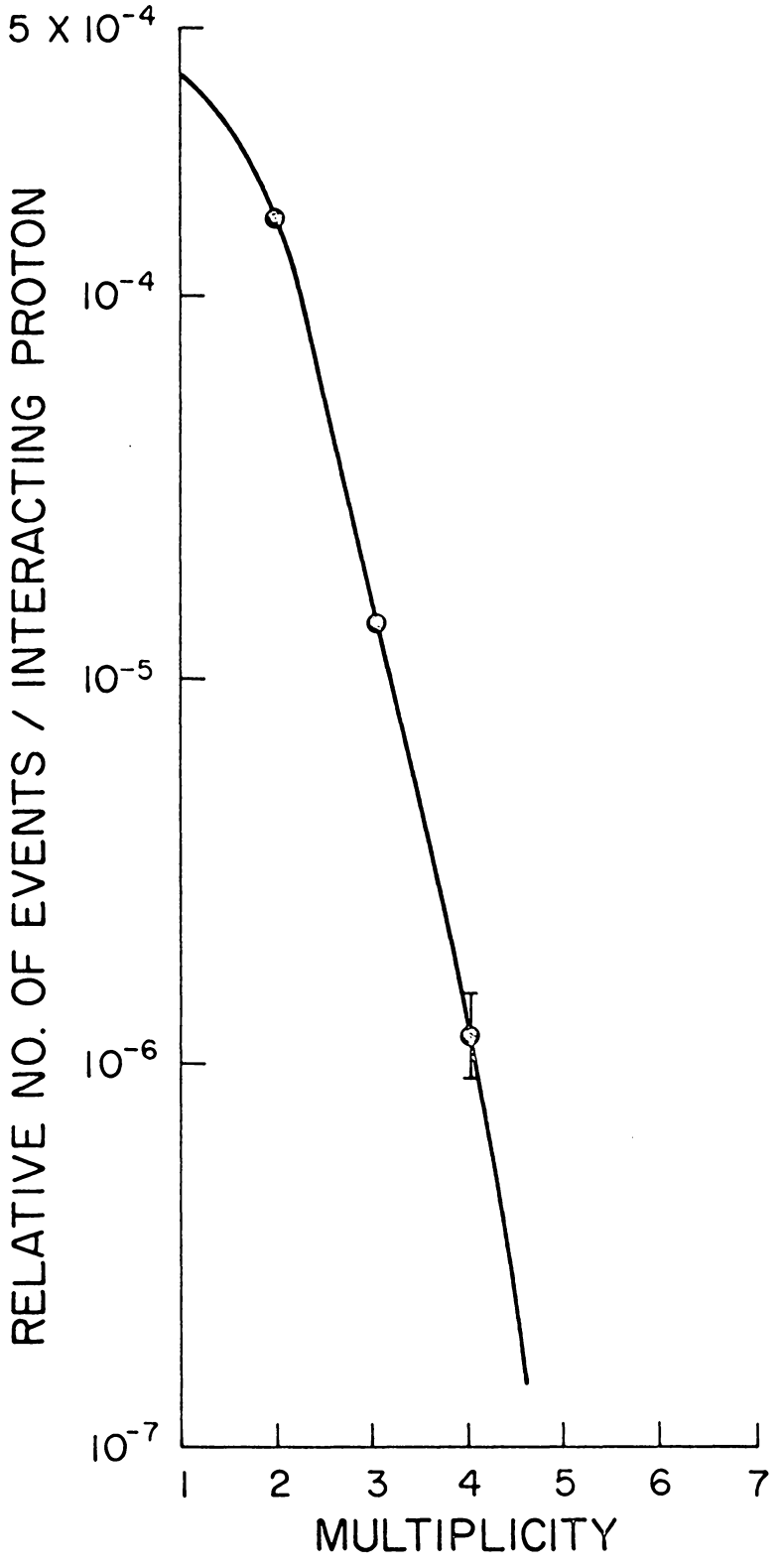

Figure 25. Multiplicity Distribution of Photons From π^0's.

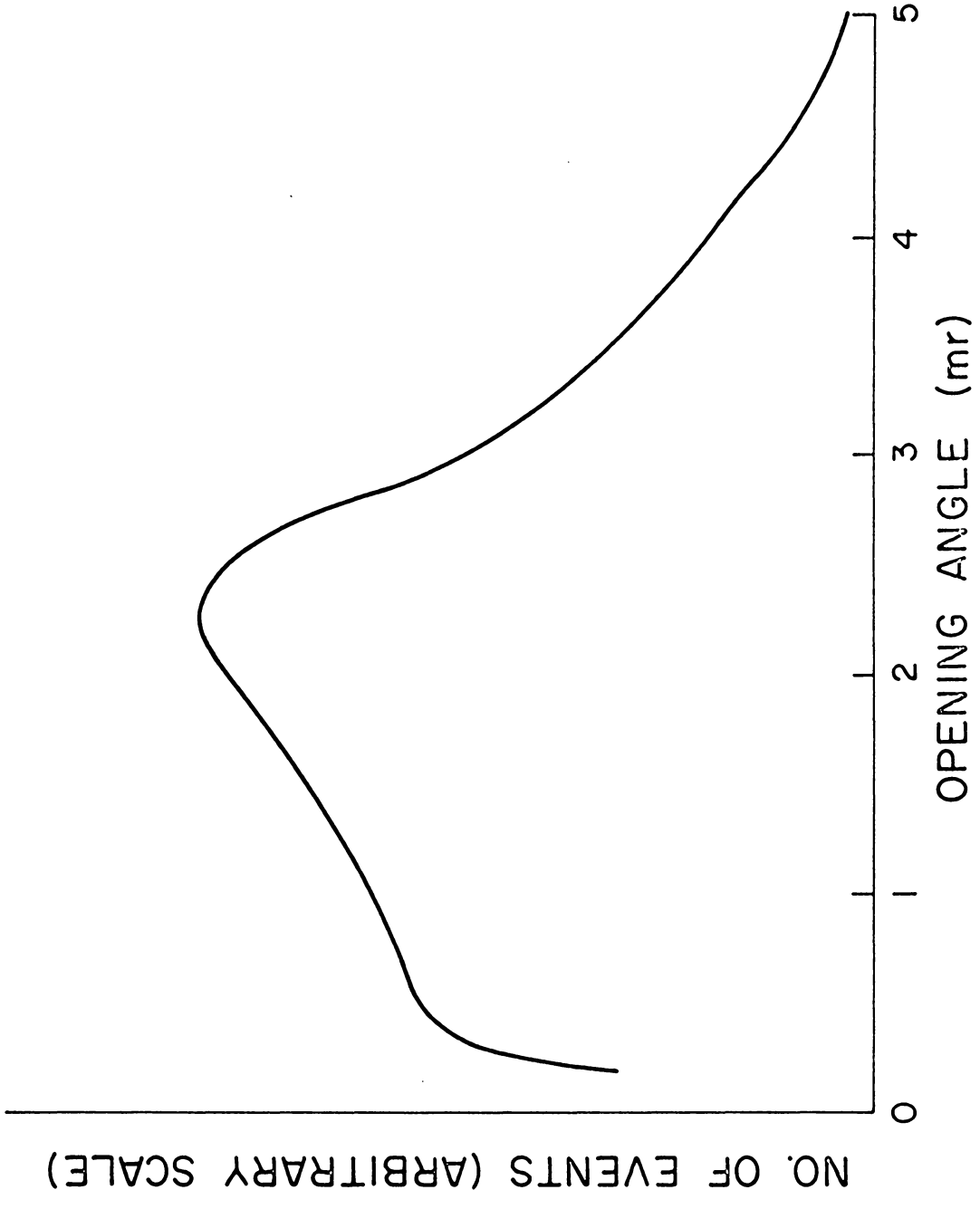

Figure 26. Angular Distribution of Photons From π^{o}'s.

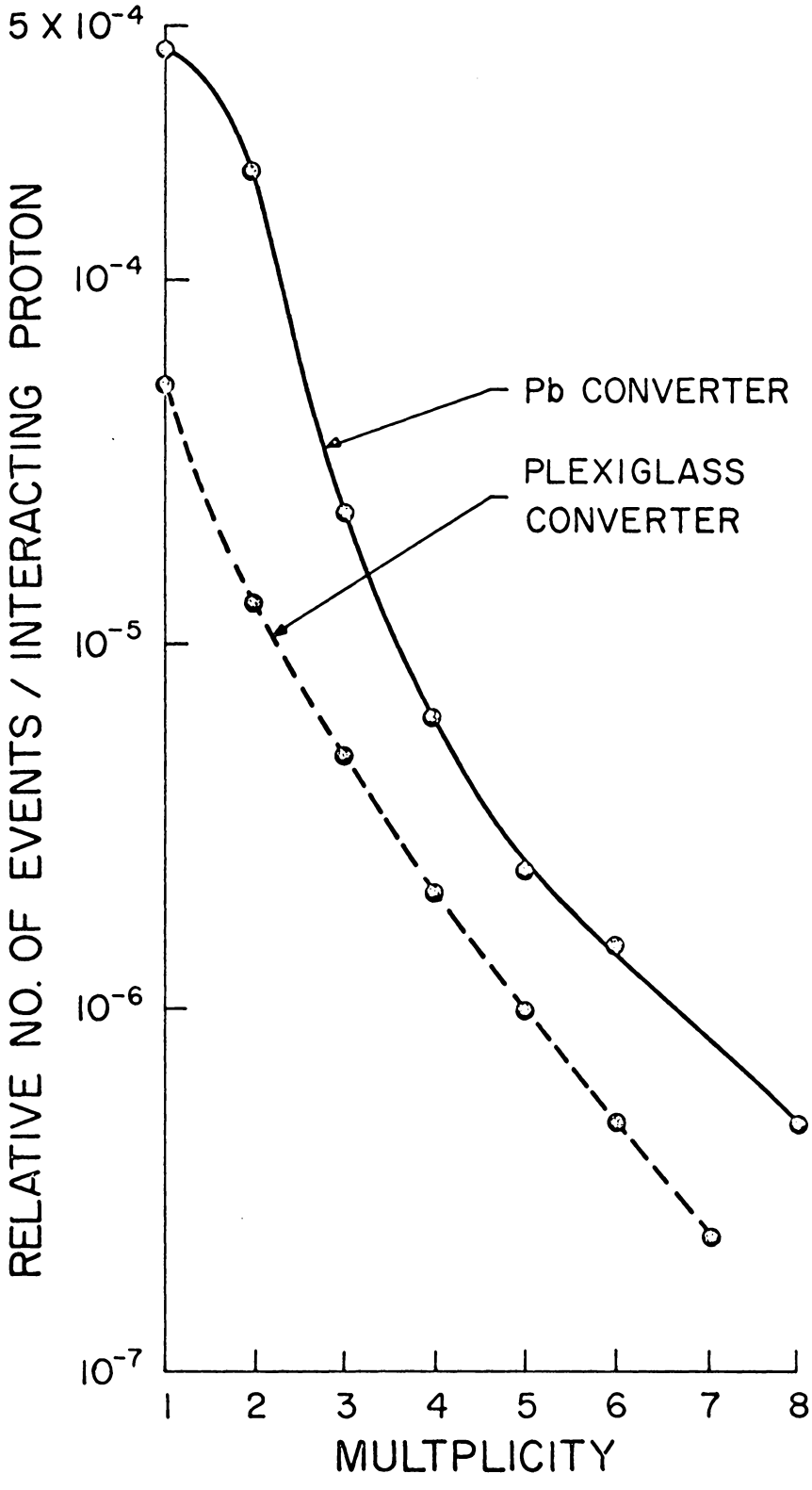

Figure 27. Multiplicity Distributions in Plexiglass and Lead.

The vita has been removed from the scanned document

SEARCH FOR MULTI-PHOTON EVENTS FROM pp INTERACTIONS AT 300 GeV/c

by

Donald Meade Stevens

(ABSTRACT)

Using a detector developed in a VPI-BNL collaboration, we have searched for multi-photon events from pp interactions at 300 GeV/c. We measured the multiplicity, energy and angular distributions of approximately 340,000 events. Of the 80,000 events that have been analysed, the angular distributions are consistent with photon production by known processes. The energy distribution of photons shows a rise in cross-section at approximately 150 GeV, an anomaly which can not be explained by known processes.